Journal of Building Engineering 114 (2025) 114381

Contents lists available at ScienceDirect

Journal of Building Engineering

journal homepage: www.elsevier.com/locate/jobe

Enhancing structural robustness of existing buildings through roof-level retrofit beams

Lisbel Rueda-García *, Brais Barros, Marcos Arias-Gracey, Juan Sebastián Fontalvo-García, Manuel Buitrago, Jose M. Adam

ICITECH, Universitat Politècnica de València, Camí de Vera s/n, 46022, Valencia, Spain

A R T I C L E I N F O

Keywords:
Structural robustness
Progressive collapse
Nonlinear dynamic analysis
Steel building
RC building

A B S T R A C T

The increasing occurrence of extreme events has underscored the importance of ensuring that existing buildings can withstand localised damage without triggering progressive collapse. Various retrofitting strategies have been proposed to enhance structural robustness, such as local strengthening of connections, bracing systems, or reinforcement of slabs and beams. However, these solutions are often invasive, difficult to implement in existing buildings, or limited in scope, as they primarily address local failure mechanisms without engaging the structure as a whole. As an alternative, roof-level retrofit beams have emerged as a promising global strategy to enhance robustness. By stiffening the roof-level beam, this solution aims to activate efficient alternative load paths in the event of a column failure. The retrofit beam assumes most of the load of the failed column that would otherwise be carried by slabs and beams above the failed column, possibly enabling their failure. The roof-level beam redistributes then the load among the connected columns, thus engaging the entire structure in a more global load-resisting mechanism. This article presents an in-depth analysis of the functioning of this retrofitting strategy through nonlinear dynamic simulations carried out on two representative case studies: a reinforced concrete and a steel building. The analysis explores the load redistribution mechanisms, the structural demands in key elements before and after retrofitting, and the system's main limitations. Different combinations of damage scenarios and retrofit beam configurations were also investigated. The article provides a foundational understanding of the structural behaviour of roof-level retrofit beams and highlights key considerations to guide their application in real structures.

1. Introduction

The frequency of extreme events is rising worldwide, with extreme weather events emerging as a dominant hazard in the 21st century [1]. Beyond natural hazards, buildings face threats from ageing, material degradation (e.g., corrosion), accidental impacts, and even armed conflicts. These threats can cause local damage to critical structural elements, making buildings vulnerable to collapse. Such damage can trigger a chain reaction of failures, leading to partial or total building collapse, a phenomenon known as "progressive collapse" [2]. As a result, structural robustness has gained importance, aiming to reduce this vulnerability by ensuring structures remain insensitive to local failures [3].

* Corresponding author.
E-mail address: lisruega@upv.es (L. Rueda-García).

https://doi.org/10.1016/j.jobe.2025.114381
Received 25 July 2025; Received in revised form 30 September 2025; Accepted 11 October 2025
Available online 16 October 2025
2352-7102/

Building robustness received little attention until the collapse of the Ronan Point apartment block (London, 1968), after which progressive collapse risk began to be incorporated into building codes and design guidelines [4,5]. However, it was only after the collapses of the Alfred P. Murrah Federal Building (Oklahoma, 1995) and the Twin Towers (New York, 2001) that widespread public concern arose, prompting the development of new standards and recommendations [3,6]. Since then, advanced regulations on structural robustness have been developed [7–11], though they remain non-mandatory in most countries. These focus on providing alternative load paths (ALPs) to redistribute loads after the loss of load-bearing elements [12]. Ongoing efforts are being made to improve these regulations and facilitate their implementation in professional practice [13].

The scientific community has shown sustained interest in this field, reflected in the growing number of annual publications on building progressive collapse [13]. Many of these studies focus on understanding the phenomenon and enhancing structural robustness at the design stage [3]. However, existing buildings remain particularly vulnerable due to their age and the fact that many were designed without considering robustness criteria, as these regulations were only introduced in recent years.

Many existing buildings approaching the end of their service life may require strengthening to enhance their robustness [14], especially essential facilities such as schools, hospitals and other high-occupancy buildings. Additionally, existing buildings changing use, particularly if their consequence level increases, must be adapted to current regulations, which may necessitate structural strengthening. Many authors have identified this need and have focused on developing retrofitting techniques for existing buildings to enhance their resistance to progressive collapse.

Numerous techniques have been proposed to prevent or mitigate initial damage. These techniques, which are primarily local in nature, are mostly threat-based. Most studies focus on fire, impact, and blast scenarios [15]. Common strengthening methods include concrete overlays and fibre-reinforced polymer (FRP) strengthening [16]. Other researchers have focused on controlling collapse propagation by adding new alternate load paths (ALPs) or enhancing existing ones. For example, strengthening connections and joints has been widely explored, both in steel structures [17,18] and in reinforced concrete (RC) structures [19,20]. Additionally, techniques have been proposed for strengthening slabs, such as using FRP [21], or beams, such as employing steel cables [22]. Some studies have also evaluated the effectiveness of bracing, mainly in steel structures [23,24], but also in RC structures [25].

As observed, a wide range of solutions has been explored in the literature. However, these interventions are often difficult to implement in existing structures due to their invasive nature or complex application. Some techniques, such as bracing, may also impact the architecture of outer walls and require a complete redistribution of a building's interior spaces. Furthermore, many of these approaches are local in nature and do not take full advantage of the overall structural capacity to activate ALPs after the failure of a load-bearing element. Consequently, there is an urgent need to develop practical and efficient solutions that enhance the robustness of existing buildings while overcoming the limitations of the most widely studied retrofitting strategies to date.

To address the aforementioned limitations, this article proposes a retrofitting technique for existing buildings that involves installing retrofit beams at the roof level connected to the existing beams and column heads. In the event of the failure of one or more columns on the lower floors, the floor slabs would be suspended from these roof-level beams, effectively activating ALPs. This solution is designed to minimise interference with the building's interior space, as most of the required construction work would be concentrated on the roof, ensuring minimal disruption to the building's functionality and layout. Moreover, this approach aims to provide a more global resistance mechanism by integrating structural elements located farther from the initial failure rather than relying solely on adjacent components. Additionally, placing the retrofit at the roof level reduces its exposure to extreme events occurring on the lower floors, such as vehicle impacts or floods. Finally, these types of interventions on the roof are generally classified as strengthening measures with negligible interference in seismic performance [15], since they do not significantly increase the structure's weight and lateral stiffness.

Similar strategies involving roof-level modifications have been explored by various authors in the literature, with a particular focus on steel buildings. Several studies have investigated the robustness of structures after adding a steel truss on top of the building, which, unlike the solution proposed in this article, is connected only to the column heads [14,26,27]. Other authors have reinforced the last floor by introducing horizontal bracing or by increasing the rigidity of the top floor connections [23,28,29]. While these studies provide valuable insights, they are often based on simplified approaches, frequently focusing on a single case study without exploring a range of retrofit strategies or configurations. In some cases, the contribution of floor slabs is not considered, or the analysis is limited to two-dimensional (2D) models. Nonetheless, all of them report improved structural robustness following the interventions.

Freddi et al. [30] further explored this topic through a detailed 2D analysis of the possible failure modes and ALPs in a case study involving a steel moment-resisting frame building strengthened with roof trusses of varying stiffness. The findings demonstrated that the proposed retrofitting solution allows for a more uniform distribution of axial forces in the columns after the column removal, while also reducing dynamic amplification effects due to the introduction of the roof-truss. Additionally, the study identified critical details that should be carefully examined when implementing this retrofitting system. For instance, excessive stiffness of the roof truss may induce significant tensile forces in the columns and connections above the removed column. The authors also highlighted that a three-dimensional (3D) analysis of these roof trusses would better assess their redistribution capacity, as a 3D truss system would distribute loads among a greater number of columns.

On the other hand, the number of studies employing roof-level modifications in reinforced concrete (RC) buildings is limited. Zahrai & Ezoddin in Ref. [31] connected the column heads of RC buildings using a steel truss, or cap-truss, arranged in a star-shaped configuration. Although their study adopts a simplified approach, it provides useful verification of the technique's effectiveness. Another innovative technique has been proposed for RC buildings, involving the use of vertical cables parallel to the columns, connected at the beam ends and hung from a steel truss at the top of the structure, which is attached to the column heads [32]. A similar solution is presented in Ref. [33] for RC buildings with flat slabs. Although both approaches achieved promising results, the practical implementation of cable connections to beams or slabs is considered highly intrusive and complex.

This article aims to evaluate the effectiveness of the proposed strengthening solution, which consists of installing retrofit beams at the roof level of buildings connected to the existing beams and column heads to enhance structural robustness. To conduct this study, nonlinear dynamic numerical simulations are performed on two case studies: an RC building and a steel building, both representative of modern construction. First, a comprehensive investigation is conducted into the structural behaviour of retrofitted buildings under a perimeter column removal scenario. Subsequently, alternative failure scenarios and retrofit beam configurations are evaluated. In this way, fundamental knowledge is gained regarding the alternative load paths occurring in low-rise buildings retrofitted with roof-level beams.

2. Description of the buildings and the retrofitting system

2.1. Characteristics of the buildings

To understand the behaviour of the proposed retrofitting system under different damage scenarios, two buildings were designed and retrofitted, one with an RC and the other with a steel structure. The retrofit roof beams were arranged in various configurations and dimensions.

Both buildings were designed according to the current European standards [10,11,34,35]. The structures were composed of beam-column frames oriented in two orthogonal directions. The floor plan included seven spans in one direction and three spans in the other, each measuring 6 m. Both buildings had three 4-m high stories resulting in a total building height of 12 m. The RC building featured concrete slabs for the floor system, while the steel building was designed with composite metal deck slabs. In addition to the self-weight, vertical actions included 2 kN/m^2 of permanent loads and 3 kN/m^2 of live loads. The design also considered horizontal loads from wind and seismic actions, representative of the central-northern inland region of Spain. This area is characterised by moderate winds, with a basic wind speed of 26 m/s [11], and low seismicity. Consequently, a low-ductility design approach was adopted. The buildings are low-rise structures that typically do not require lateral bracing or wall systems [12]. Explicit structural robustness requirements were not incorporated, as is common in existing buildings.

The columns in the structures were identified using the following nomenclature: *xy.n*, where *x* represents the position on the grid along the X-direction, identified by letters from A to H; *y* represents the position on the grid along the Y-direction, identified by numbers from 1 to 4; and *n* indicates the floor level, ranging from 1 to 3 (see Fig. 1a).

Regarding the materials employed, C30/37 concrete was used for the beams, columns, and slabs of the RC building, as well as for the slabs of the steel building. This concrete is characterised by a compressive strength of 30 MPa on cylindrical specimens, a Young's modulus of 33 GPa, and a Poisson's ratio of 0.2. The reinforcing steel bars in both buildings were made of B500 steel, featuring a yield strength of 500 MPa, an ultimate strength of 540 MPa, and a Young's modulus of 200 GPa. Additionally, in the steel building, structural steel grade S355 was employed for beams, columns, and the steel sheet of the composite metal deck, with a Young's modulus of 210 GPa, a Poisson's ratio of 0.3, a yield strength of 355 MPa, and an ultimate strength of 490 MPa.

Regarding the structural configuration of the RC building, 350 × 350 mm columns were used throughout the ground floor, while the remaining columns in the structure had a cross-section of 300 × 300 mm. The beams were uniformly 300 × 300 mm across the entire building, and the slabs had a thickness of 200 mm. The structure was assumed to be cast in situ, ensuring rigid connections between elements. Reinforcement details are given in the Supplementary Materials.

In contrast, in the steel building, IPE profiles were used for the beams, ranging in depth from 240 mm to 450 mm, while HEM profiles, with depths between 100 mm and 240 mm, were employed for the columns (the dimensions of each profile are provided in the Supplementary Materials). The column profiles were arranged so that beams in the building's longer direction (X-direction) were fully connected to the column flanges. Conversely, only the beams' webs were connected to the column webs in the shorter direction (Y-direction), which resulted in limited flexural strength (see Fig. 1b). The composite steel decks consisted of a 0.8 mm thick, 60 mm high trapezoidal steel sheet, which was topped with a 100 mm thick layer of concrete.

Although the buildings were not originally designed to meet the structural robustness requirements of current robustness standards, it was verified that their designs complied with the prescriptive rules of EN 1991-1-7 [11], which ensure the horizontal and

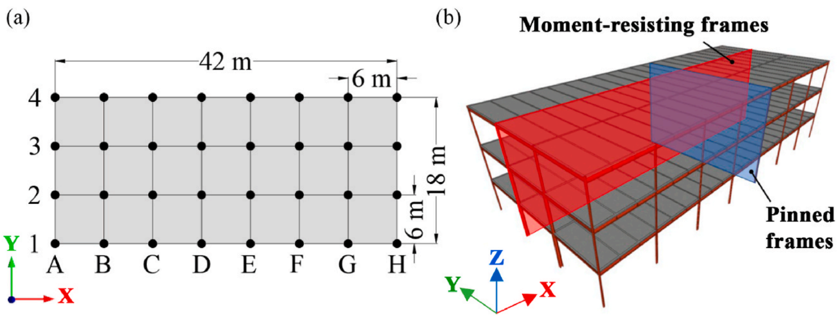

Fig. 1. (a) Identification of column grid alignments in the buildings under study; (b) 3D representation of the location of moment-resisting frames and pinned frames in the studied steel buildings.

vertical tying of structural elements.

2.2. Characteristics of the retrofitting system

The retrofitting system for the RC buildings of this study was designed as cast-in-place concrete beams placed over the existing beams (see Fig. 2a). In reality, these beams would be connected to the existing beams and column heads by drilling the existing concrete and installing dowels or studs, creating a connection as continuous as possible along the entire beam to promote the joint action of both structural elements. In the steel buildings of this study, a steel beam was welded to the existing steel beams and column heads for simplicity, resulting in a continuous connection (Fig. 2b). In practice, connecting both beams will require modifying the floor slab placed over the existing beams. The reproduction and the connection method between these original and additional elements are outside the scope of this study.

This study utilises retrofit beams with various dimensions and configurations to compare their effectiveness (in practice, the design of the retrofitting system would involve selecting the optimal beam dimensions to prevent structural collapse for all considered failure scenarios). Specifically, for reinforced concrete buildings, two different sizes of retrofit beams were employed on top of the existing beams: one with a depth equal to the height of the existing beam (H), resulting in a total roof beam depth of 2H, and another with a depth three times that of the existing beam, yielding a total depth of the roof beam of 4H (see Fig. 2b). For steel buildings, specific structural profiles were selected to achieve an increase in moment of inertia (with respect to the centroid of the cross-section) equivalent to that provided by the 2H and 4H retrofitting configurations in concrete structures; therefore the 2H and 4H nomenclature is retained for consistency. In both cases, the original IPE 360 profile was maintained. For the 2H configuration, an additional IPE 450 profile was attached, while for the 4H configuration, a built-up steel section with a total height of 1080 mm was added (see Fig. 2b).

Both retrofits (2H and 4H) are conceived in three different configurations: placed on the perimeter beams at the roof (RP), placed on the perimeter beams and all Y-direction beams at the roof level (RY), and placed on the perimeter beams and all X-direction beams at the roof level (RX), as illustrated in Fig. 3. Section 4 presents a detailed study on the effectiveness of the retrofit using the RP configuration, whilst the other configurations are analysed in Section 5.

In practice, the retrofitting system could also be implemented as a steel truss connected to the column heads of the structure, as reported in the literature [14,26,27,31], if deemed appropriate by the designer. In this case, the capacity of the existing beams would not be utilised, and the load transfer would rely solely on these discrete connections. However, in cases where the existing beams are too weak and require significant strengthening to withstand the design forces of the retrofit, the steel truss solution could be a viable alternative.

3. Description of the numerical modelling

3.1. General characteristics of the numerical modelling

The resistance of buildings to progressive collapse has a distinctly three-dimensional nature; therefore, it was deemed important to

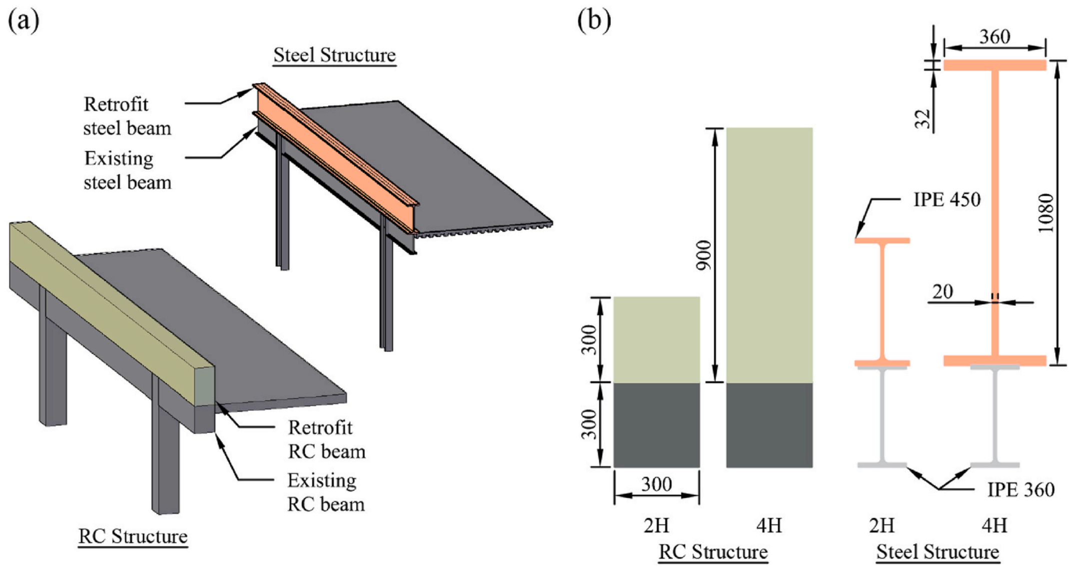

Fig. 2. (a) Representation of the proposed retrofitting system in an RC building and a steel building; (b) 2H and 4H retrofits in RC and steel buildings.

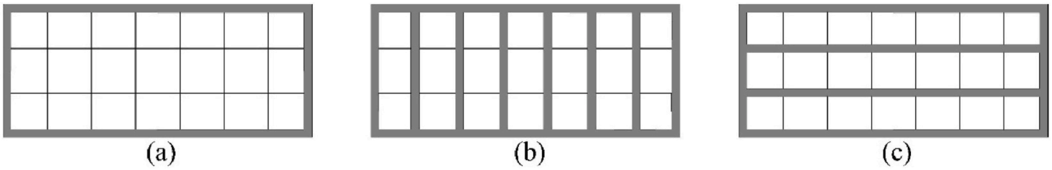

Fig. 3. Different configurations of the roof retrofit beams: (a) RP; (b) RY; (c) RX.

develop 3D models of the buildings to account for the 3D framing effect. Additionally, the contribution of floor systems in providing alternative load paths is well recognised [36,37]. Consequently, the models included not only the 3D frames but also the slabs.

The progressive collapse of buildings is a complex phenomenon involving the nonlinear behaviour of materials, large deformations, and dynamic effects [3]. Current codes and guidelines allow for both linear and nonlinear analyses. However, nonlinear simulations are more accurate as they can capture the structural behaviour up to the point of failure. This is the approach adopted in this study, which accounts for both material and geometric nonlinearities, including concrete cracking and crushing, as well as the yielding and fracture of reinforcement bars under large deformations [12]. In this study, dynamic nonlinear numerical models of the buildings were chosen, as they are more realistic than static models because they account for dynamic effects, which amplify the forces and deformations experienced by the system when load-bearing elements are suddenly removed.

The dynamic nonlinear analysis performed consisted of two phases. In the first phase, the load F_d was statically applied to all the floors of the structure. The combination of actions for accidental design situations was used, as specified in EN 1990:2023 [10], incorporating the combination factors shown in Eq. (1):

$$F_d = \sum_i G_{k,i} + 0.7Q_k \tag{1}$$

where $G_{k,i}$ is the characteristic value of the permanent action i and Q_k is the characteristic value of the live load.

In the second phase, the load-bearing element corresponding to the considered damage scenario is removed (various failure scenarios included in the current robustness regulations are analysed in this study, as shown in Section 4 and Section 5). A constant viscous (modal) damping ratio of 2 % was adopted for all analyses [38]. A removal time of 0.02 s was used, which is less than one-tenth of the predominant vertical vibration mode of the structural system [7]. The total simulation time was 5 s.

3.2. Particularities of the reinforced concrete building model

The software used for modelling the RC building was the FEM software SAP2000 [39], employing a practical modelling strategy in this software that was proposed and thoroughly validated by Setiawan et al. in Ref. [12]. Details of this validation are provided in the Supplementary Materials.

Beams and columns were represented as line elements, where nonlinearity due to cracking and reinforcement yielding was captured using the distributed-fibre approach [40]. Different cross-sections were assigned to the elements to account for variations in reinforcement along the same element. P-M2-M3 fibre hinges were employed to model the nonlinear axial behaviour of a series of fibres distributed across the entire cross-section of the elements. These hinges were placed at multiple cross-sections of columns and

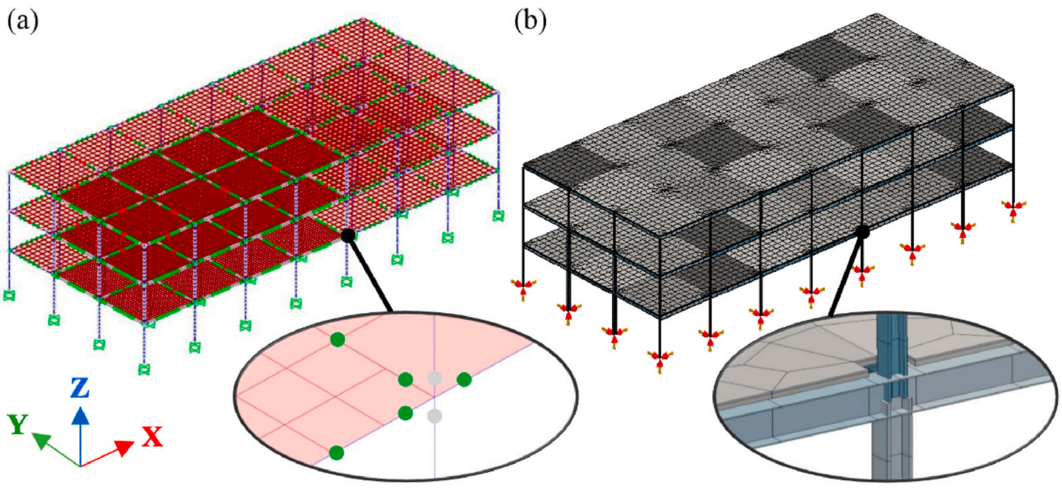

Fig. 4. (a) Representation of the numerical model of the RC buildings developed in SAP2000; (b) Representation of the numerical model of the steel buildings developed in DIANA FEA.

beams, following the distributed plastic hinges modelling approach [12]. A higher density of hinges was used in regions near the failing elements to enhance accuracy. The number of hinges used was based on the sensitivity analysis conducted by Setiawan et al. [12]. Specifically, 20 and 10 plastic hinges were placed in beams and columns near the failing element, respectively, and 10 and 5 hinges in beams and columns far from the failing element, respectively. The higher and lower densities of plastic hinges can be observed in the numerical model representation shown in Fig. 4a.

The floors of the structure were modelled as nonlinear-layered shells (*Shell – Layered/Nonlinear*), allowing for the inclusion of slab reinforcement in both directions and accounting for the nonlinear behaviour of concrete and steel. Mesh refinement was applied in the vicinity of the failing elements (squares with a side length of $L/20$ m, where L is the centreline-to-centreline distance between two adjacent columns), whereas a coarser mesh ($L/10$ m) was adopted for the rest of the structure (see Fig. 4a). The optimal mesh size, which provides accurate and reliable results with a reasonable computation time, was also based on the analysis carried out in Ref. [12].

The beams of the retrofitting system, together with the existing beams, were modelled as single elements, with the dimensions and mechanical properties derived from the composite cross-section. These line elements were modelled as linear elastic, assuming that their reinforcement is adequately designed to remain within the elastic and linear regime during the local failure of a load-bearing element. This modelling strategy makes it possible to avoid reinforcement design based on force envelopes for different failure scenarios, which would otherwise be required if nonlinear elements were defined, or even strengthening the existing beam to withstand the design forces.

The numerical models do not explicitly simulate shear failure mechanisms, since flexure is expected to be the predominant mechanism, and accounting for it would significantly increase the computational cost. Instead, shear capacity is assessed in a post-processing phase. For the structures analysed, shear resistance was not found to be a governing or limiting factor.

The dynamic time-history response of the RC building model was analysed using the Newmark method ($\gamma = 1/2$, $\beta = 1/4$), with a constant integration time step of 0.01 s.

3.3. Particularities of the steel building model

The steel building was modelled using the FEM software DIANA FEA [41], which was particularly suitable for representing the composite steel deck slabs with the desired level of detail. The modelling strategy was adequately validated, and details of this validation are provided in the Supplementary Materials. A representation of the model is shown in Fig. 4b.

Beams and columns were modelled as 'Class-III Beams 3D' elements, using the respective profile cross-section and elastoplastic steel material properties. The default integration points used by DIANA were retained, as they offer a good balance between computational cost and accuracy. Fully rigid connections were assigned throughout the structure, except for the beam-to-column connections along the shorter (Y) direction. These were modelled as pinned connections according to the design specifications, resulting in connections with no flexural capacity.

The floors were modelled using a combination of line and shell elements to accurately capture the composite deck's structural behaviour. Line elements were used for the secondary beams supporting the composite deck. The deck was represented using shell elements, incorporating the concrete slab, the top reinforcement, and the steel sheet, which was modelled as an equivalent bottom reinforcement layer. A rigid connection was assigned between the secondary beams and the shell elements. Further details on this approach can be found in the Supplementary Materials.

Regarding the mesh properties, the beam elements were modelled as two-node, three-dimensional Class III beam elements. The shell elements were represented using four-node quadrilateral isoparametric curved shells. A mesh sensitivity analysis was conducted to determine an appropriate element size, and a mesh size of 600 mm was selected as it provided a good balance between computational cost and numerical accuracy.

Unlike the RC building model, the beams of the retrofitting system were modelled as nonlinear elements, like the rest of the line elements in the building, and were placed on top of the existing roof beams. For this study, the connection between the existing beams and the retrofit beams was modelled as rigid.

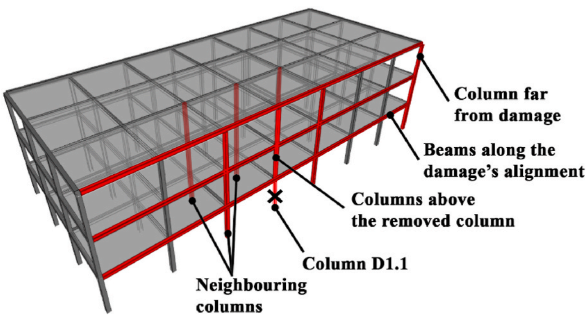

Fig. 5. Elements analysed in Section 4.2: key structural elements most affected by the addition of perimeter roof-level retrofit beams for the removal of column D1.1.

The Newmark integration algorithm ($\gamma = 1/2, \beta = 1/4$) was used. Since DIANA FEA allows variable time steps, they were adopted to ensure the required accuracy: 100 steps of 0.005 s, 50 steps of 0.01 s, and 80 steps of 0.05 s.

4. Understanding the role of the roof-level retrofit beams

4.1. Methodology

To perform a conceptual analysis of the behaviour of the roof-level retrofit beams, a detailed investigation is carried out on a failure scenario for both the RC and steel buildings. The U.S. standard UFC 4-023-03 [7] defines a series of single-column removal scenarios, considering internal, corner and edge column locations. This section analyses one specific case: the failure of an edge column located at the midpoint of the building's long side on the ground floor (column D1.1, see Fig. 5). This initial focus allows for an in-depth understanding of the retrofit behaviour under a representative and critical scenario. The roof retrofitting layout selected for this analysis is the perimeter configuration (RP), considering both beam depths (2H and 4H). Additional failure scenarios and retrofitting configurations will be examined later in Section 5.

The methodology employed in this section to assess the effectiveness of the retrofitting technique begins with an analysis of the dynamic response of the structures after the removal of column D1.1. Subsequently, load redistribution is examined based on the vertical reactions at the building foundations. Next, the key structural elements that could experience the most significant changes in demand due to the incorporation of the roof-level retrofit beams are identified, and a detailed analysis of the main internal forces governing these elements is conducted. Specifically, the study focuses on the columns above the removed column, the neighbouring columns, a column located far from the damaged area, and both the retrofit and regular beams across the three stories of the building within the XZ plane where the removed column is located (Fig. 5). Based on the analysis of these results, a comprehensive synthesis of the structural behaviour of the retrofitted buildings is provided.

4.2. Analysis of key structural elements

4.2.1. Dynamic response

Fig. 6a presents the dynamic response of the three analysed reinforced concrete (RC) buildings: without retrofit (CB-NR), with perimeter retrofit using a total depth of 2H (CB-RP-2H), and with perimeter retrofit using a depth of 4H (CB-RP-4H). The displacement at the nodes located above the removed column D1.1 on floors 1, 2, and 3 is plotted against time. This parameter is selected as it represents the demand level across the storeys, with lower demand corresponding to reduced displacement of the nodes located above

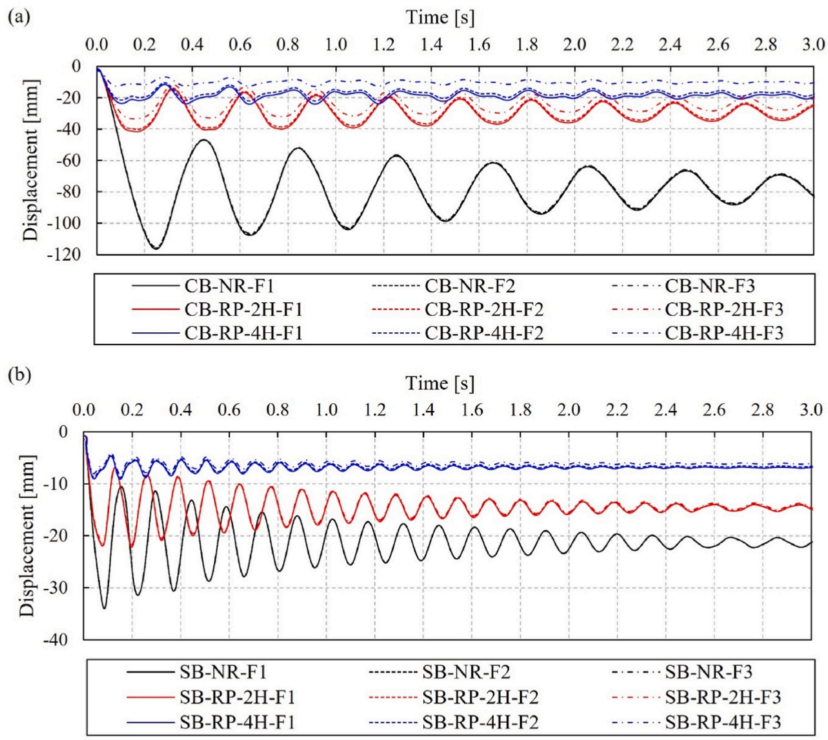

Fig. 6. Displacement at the nodes located above the removed column on floors 1, 2, and 3 (F1, F2 and F3) over time for different buildings: (a) Reinforced concrete buildings: CB-NR, CB-RP-2H, and CB-RP-4H; (b) Steel buildings: SB-NR, SB-RP-2H, and SB-RP-4H.

the removed column. Fig. 6b shows the corresponding results for the steel buildings (SB-NR, SB-RP-2H, and SB-RP-4H). As observed in the graphs, in none of the analysed buildings did the column removal lead to structural collapse, which would be evidenced by a displacement that continuously increases throughout the simulation.

The graph in Fig. 6a shows that the retrofitted buildings exhibit a significantly stiffer response (lower peak displacement, δ_{peak}) compared to the non-retrofitted building. Furthermore, it is observed that in building CB-NR, the displacement at the nodes of the three floors is similar (only 1.4 mm difference between the peak displacements of floors 1 and 3). In contrast, as expected, in the retrofitted buildings, the floor with the retrofit beams (floor 3) exhibits a much smaller displacement than the lower floors due to its increased stiffness. This difference is more pronounced when the retrofit beams are larger: 8.4 mm between floors 1 and 3 in building CB-RP-2H (20 %, as shown in Table 1) compared to 10.5 mm in building CB-RP-4H (45 %).

In the steel buildings (Fig. 6b), the displacements observed after column removal are generally much smaller than those in the RC buildings. Although steel buildings are typically more flexible, in this case the adopted configuration and design assumptions, including the consideration of lateral loads, absence of bracing, and the distribution of moment-resisting and pinned frames, resulted in a stiffer steel structure. As with the RC buildings, the retrofitted steel structures exhibit greater stiffness; however, the SB-RP-2H retrofit does not achieve as significant an improvement as in the concrete building. On one hand, the peak displacement of SB-RP-2H is reduced by 35 % compared to the non-retrofitted building (see Table 1), whereas the reduction in CB-RP-2H is 64 %. On the other hand, the third floor of SB-RP-2H shows a peak displacement very similar to that of floors 1 and 2 (only 2 % difference between floors 1 and 3). In contrast, the building with the 4H retrofit shows very similar results to those of the concrete building with the same retrofit: the peak displacement of SB-RP-4H is reduced by 73 % compared to the non-retrofitted case, while the reduction for the RC building is 80 %. In addition, the third floor of the steel building exhibits a smaller displacement than the other floors, with only 1.0 mm difference between floors 1 and 3 (11 %).

When damping ratios are derived from the dynamic response curves using the logarithmic decrement method [42,43], it is observed that the original systems without retrofit beams, in both the RC and steel buildings, exhibit higher damping ratios (0.31 % and 0.36 %, respectively). As the stiffness of the retrofit increases, a slight decrease in damping is noted. For example, CB-RP-2H and CB-RP-4H show similar damping values of 0.18 % and 0.15 %, respectively. The same trend is observed in the steel building, where SB-RP-2H and SB-RP-4H exhibit damping ratios of 0.22 % and 0.19 %, respectively. Overall, all steel systems demonstrate damping values of the same order of magnitude as the RC systems, but with slightly higher damping.

Additionally, it is worth noting that the most heavily retrofitted buildings (CB-RP-4H and SB-RP-4H) exhibit a distinct dynamic response. The dynamic response deviates from the expected sinusoidal pattern, exhibiting nonlinear or distorted characteristics, likely resulting from a decoupling of the structure into two dynamically distinct sub-systems. This behaviour may be related to the stiffness difference between the upper floor and the lower floors, which could cause them to vibrate at slightly different frequencies. At the onset of failure, the three floors appear to behave as a unified system. However, the upper floor seems to reach its maximum displacement slightly earlier than the others (this is clearly observed in Fig. 6a, where the first peak displacement is reached by CB-RP-4H-F3 at 0.08 s, while CB-RP-4H-F1 and -F2 reach it at 0.10 s), since its higher stiffness may lead to smaller displacements and higher natural frequencies, potentially resulting in a shorter vibration period. As a result, the floor with the retrofitted beam might begin to move upward while the other floors are still descending. This out-of-phase motion could indicate a partial loss of synchrony between floors, an effect that should be considered in the design of the retrofitting system.

In conclusion, the 4H retrofitting configuration proved to be highly effective in both concrete and steel buildings, significantly enhancing structural performance. However, special attention should be given to the potential dynamic decoupling observed in the most heavily retrofitted cases, which should be carefully addressed in the retrofitting design. By contrast, the 2H retrofit was found to be considerably more effective in the concrete building than in the steel one.

4.2.2. Vertical reactions at the supports

This section aims to investigate how retrofit beams distribute loads by analysing the vertical reactions at the supports of the buildings. Fig. 7 presents the vertical reactions of the concrete buildings at the time step corresponding to the peak displacement ($\delta_{peak,F1}$). The figure includes the undamaged building (UD), defined as the building at the end of the first load phase (as explained in Section 3.1); the building with a missing column D1.1 and non-retrofitted (NR); the building with a perimeter retrofit of depth 2H (RP-2H); and the building with a perimeter retrofit of depth 4H (RP-4H). Fig. 8 shows the corresponding results for the steel buildings. The colours displayed in the graphs result from the interpolation of values between columns, which helps to visualise the force flow.

Fig. 7a shows a typical load distribution in a building subjected to uniform loading across all its floor slabs. The removal of column

Table 1
Overview of dynamic behaviour metrics for RC and steel buildings.

Building ID	$\delta_{peak,F1}$ [mm]	$\Delta\delta_{peak}$ RP vs NR [%]	$\delta_{peak,F2}$ [mm]	$\Delta\delta_{peak}$ F2 vs F1 [%]	$\delta_{peak,F3}$ [mm]	$\Delta\delta_{peak}$ F3 vs F1 [%]	ζ [%]
CB-NR	−116.0	–	−115.9	0	−115.2	−1	0.31
CB-RP-2H	−42.0	−64	−40.3	−4	−33.6	−20	0.18
CB-RP-4H	−23.4	−80	−22.2	−5	−12.9	−45	0.15
SB-NR	−34.0	–	−34.0	0	−34.1	0	0.36
SB-RP-2H	−22.2	−35	−22.0	−1	−21.7	−2	0.22
SB-RP-4H	−9.1	−73	−8.8	−3	−8.1	−11	0.19

Notation: δ_{peak} denotes the peak displacement; F1, F2 and F3 refer to the 1st, 2nd, and 3rd floors, respectively; ζ represents the damping ratio calculated using the logarithmic decrement method.

D1.1 (Fig. 7b) causes a significant increase in axial load on the columns located along the column alignments D2, C1, and E1. A slight decrease in base reactions can also be observed in columns located along the perimeter of the structure, on the opposite side to the removed column, particularly in columns C4, D4, and E4. The remaining columns exhibit similar vertical reactions to those of the undamaged building.

The vertical base reactions of the columns after the implementation of the perimeter retrofit RP-2H (Fig. 7c) do not differ significantly from those observed in the non-retrofitted building (Fig. 7b). The main differences include an increase in axial load at the bases of columns C2 and E2, and at perimeter columns, such as C4, D4, and E4, which experienced a slight unloading in the non-retrofitted configuration (CB-NR).

The most significant change is observed in the building retrofitted with RP-4H (Fig. 7d). In this case, column D2 carries a considerably lower load compared to the other buildings without column D1.1. Furthermore, the remaining interior columns exhibit base reactions very similar to those of the undamaged structure, despite the absence of element D1.1. A slight increase in load is also observed in the perimeter columns, as the central area load is redistributed toward the stiffer regions of the structure. Overall, the load distribution along the perimeter is very similar to that of the undamaged building (Fig. 7a), with RP-4H producing slightly higher reactions at the corner columns. These results demonstrate that RP-4H retrofit can redistribute the load from the failed element to regions of the structure located away from the damaged area.

For the steel buildings, Fig. 8b shows that the removal of column D1.1 increases the load on columns D2, C1, and E1, similar to what was observed in the concrete structure. However, the increase in vertical base reaction experienced by column D2 in the non-retrofitted steel building (SB-NR) compared to the undamaged building (SB-UD) is only 19 %, significantly lower than the 48 % increase observed in the concrete counterpart (CB-NR vs. CB-UD). In contrast, columns C1 and E1 exhibit a greater increase in load in the steel structure than in the concrete one; approximately 117 % in SB-NR versus 85 % in CB-NR, with respect to the undamaged buildings. This behaviour is attributed to the weak connections in the shorter (Y) direction of the steel building, as discussed in Section 3.3, and to the smaller profiles of the beams in that direction. As a result, force transmission in this direction is less efficient than in concrete buildings, where all joints are rigid and the beam dimensions and reinforcement are equal or comparable.

Regarding the implementation of retrofitting in the steel building, Fig. 8c shows that the RP-2H retrofit presents similar results to those of the non-retrofitted structure (SB-NR). The main difference is a slight decrease in the reaction at column D2, which is about 4 % lower compared to the non-retrofitted configuration (Fig. 8b). As noted in the previous section, the RP-2H retrofit has a lower structural effect in steel than in RC. In contrast, the introduction of RP-4H retrofit (Fig. 8d) leads to a more substantial change. The most notable difference is observed in the reaction at column D2, which reaches a value comparable to that of the undamaged building (Fig. 8a). A slight increase in the base reactions of the perimeter columns is also evident. This increase is particularly significant in columns B1 and F1, where the reactions rise by 34 % and 47 %, respectively, compared to the non-retrofitted steel building (SB-NR). As observed in the concrete structure, the reactions in the SB-RP-4H building are very similar to those of the undamaged configuration (SB-UD, Fig. 8a), with a slight increase in the perimeter reactions due to the load redistribution provided by the perimeter retrofitting.

These results suggest that, as expected, greater stiffness of the retrofit beams enables the involvement of structural elements located farther from the damaged area. This allows the strengthening solution to make better use of the system's overall capacity, giving this technique a more global structural effect.

4.2.3. Columns above the removed column

Fig. 9 shows the axial force in the columns along alignment D1 across all floors, for both RC and steel structures, in the four cases

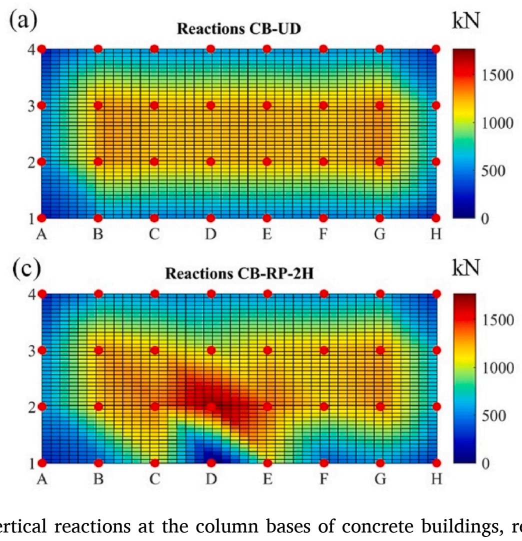

Fig. 7. Vertical reactions at the column bases of concrete buildings, represented in a plan view using a colour legend and expressed in kN: (a) Undamaged building (CB-UD); (b) Damaged and non-retrofitted building (CB-NR); (c) Damaged and retrofitted with 2H perimetral retrofit (CB-RP-2H); (d) Damaged and retrofitted with 4H perimetral retrofit (CB-RP-4H).

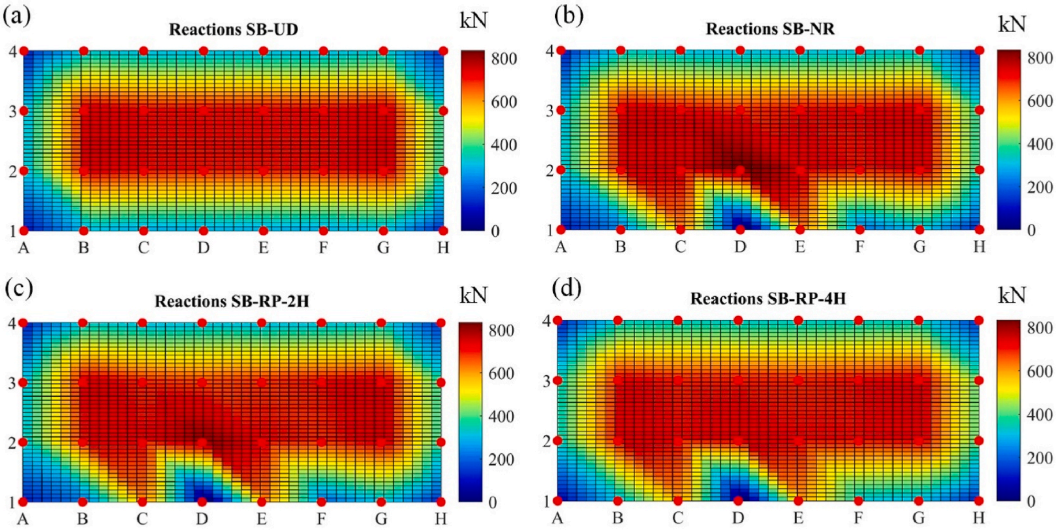

Fig. 8. Vertical reactions at the column bases of steel buildings, represented in a plan view using a colour legend and expressed in kN: (a) Undamaged building (SB-UD); (b) Damaged and non-retrofitted building (SB-NR); (c) Damaged and retrofitted with 2H perimetral retrofit (SB-RP-2H); (d) Damaged and retrofitted with 4H perimetral retrofit (SB-RP-4H).

analysed at the time when the peak displacement $\delta_{peak,F1}$ is reached: the undamaged building before the removal of column D1.1 (UD), the building with column D1.1 removed and no retrofit (NR), the building with a perimeter retrofit of depth 2H (RP-2H), and the building with a perimeter retrofit of depth 4H (RP-4H).

In the non-retrofitted buildings (CB-NR and SB-NR), following the removal of the column, the uniform flexural stiffness of all floors results in the columns located above the removed element being effectively unloaded (compressive forces close to zero). In the retrofitted buildings, however, significant tensile forces develop in the columns above the removed column due to the presence of a highly rigid roof beam. These columns transfer the load previously carried by the failing column to the retrofit beam, which in turn redistributes the load to other columns within the structure. For both concrete and steel buildings, differences in tensile forces were observed in the columns above the removed column between the RP-2H and RP-4H retrofitted cases. The greater the stiffness of the retrofit, the higher the tensile forces in the columns. This difference in tensile response between RP-2H and RP-4H is less pronounced in concrete than in steel, once again highlighting that the RP-2H retrofit had a greater effect in RC than in steel when compared to RP-4H.

The variation in the axial force of the columns provides insight into which elements are most likely to fail due to the introduction of retrofit beams. In retrofitted buildings, the columns located above the removed column experience significant tensile forces. In the steel structure, the tensile strength of the column itself is typically not a concern. In concrete buildings, however, the tensile forces may approach the tensile capacity of the columns, which depends almost entirely on the strength of the reinforcing steel and its detailing (e.g. splices). In the case study, tensile forces of up to 353 kN were observed (in CB-RP-4H), while the capacity of the reinforcement was estimated at 434 kN (using an ultimate strength of 540 MPa and excluding safety factors). Consequently, assessing the tensile strength of the columns becomes a critical step during the design of the retrofit beam, as highly rigid beams may exceed the load-carrying capacity of this load path. Nevertheless, the results obtained in this case study demonstrate that the proposed solution is viable, as the tensile capacity of the elements was never exceeded.

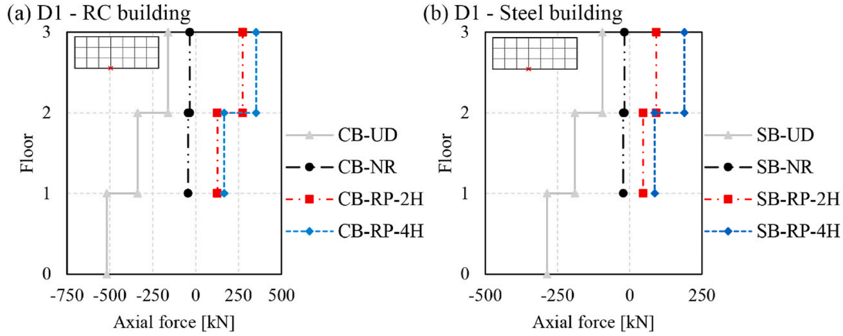

Fig. 9. Axial force in the columns of alignment D1: (a) Reinforced concrete building; (b) Steel building.

4.2.4. Neighbouring columns

Fig. 10 shows the axial forces in the columns of various alignments at the time step corresponding to the peak displacement $\delta_{peak,F1}$ in each building. Specifically, the results are presented for alignments C1, C2, and D2, which are adjacent to the removed column D1.1. Axial forces for alignments E1 and E2 are not shown due to their similarity with those of C1 and C2, respectively.

First, the behaviour of the columns along alignment C1, located at the perimeter of the building, is examined (see Fig. 10a and d). When comparing the undamaged building (UD) with the non-retrofitted building without column D1.1 (NR), it is observed that the removal of the column leads to a significant increase in axial force in the columns of alignment C1, both in the RC and the steel structure buildings. On the other hand, the installation of the perimeter retrofit of depth 2H (RP-2H) introduces high compressive forces in the upper-storey columns located at the building perimeter, adjacent to the removed column, due to the considerable internal forces acting on these elements since they are connected to the retrofit beams (see Section 4.2.6). A stiffer strengthening system (RP-4H) transmits even greater compressive forces to these elements. However, at the base of the C1 column alignment, the axial force is similar to that observed in the NR building for both strengthening schemes. As such, the variation in axial load could go unnoticed if only vertical base reactions are considered. This behaviour is attributed to the load distribution from floor to floor through beams and slabs. This highlights the importance of checking the capacity of upper-storey columns when employing the proposed retrofitting solution.

Regarding alignment D2, located in the interior of the building, a comparison between the undamaged building (UD) and the non-retrofitted building (NR) reveals an increase in axial force in the columns, both in the RC and steel buildings (see Fig. 10c and f). On the other hand, when RP-2H is implemented, the load transmitted towards alignment D2 remains very high, comparable to that of the non-retrofitted building, in both RC (Fig. 10c) and steel buildings (Fig. 10f). This suggests that the RP-2H retrofit is not particularly effective in redistributing the load towards other areas of the structure. In contrast, the use of the RP-4H retrofit results in axial forces in the D2 alignment columns that are very similar to those in the undamaged building, both in the RC and steel structures.

Finally, regarding the columns along alignment C2, located in the interior of the building along the diagonal from the removed

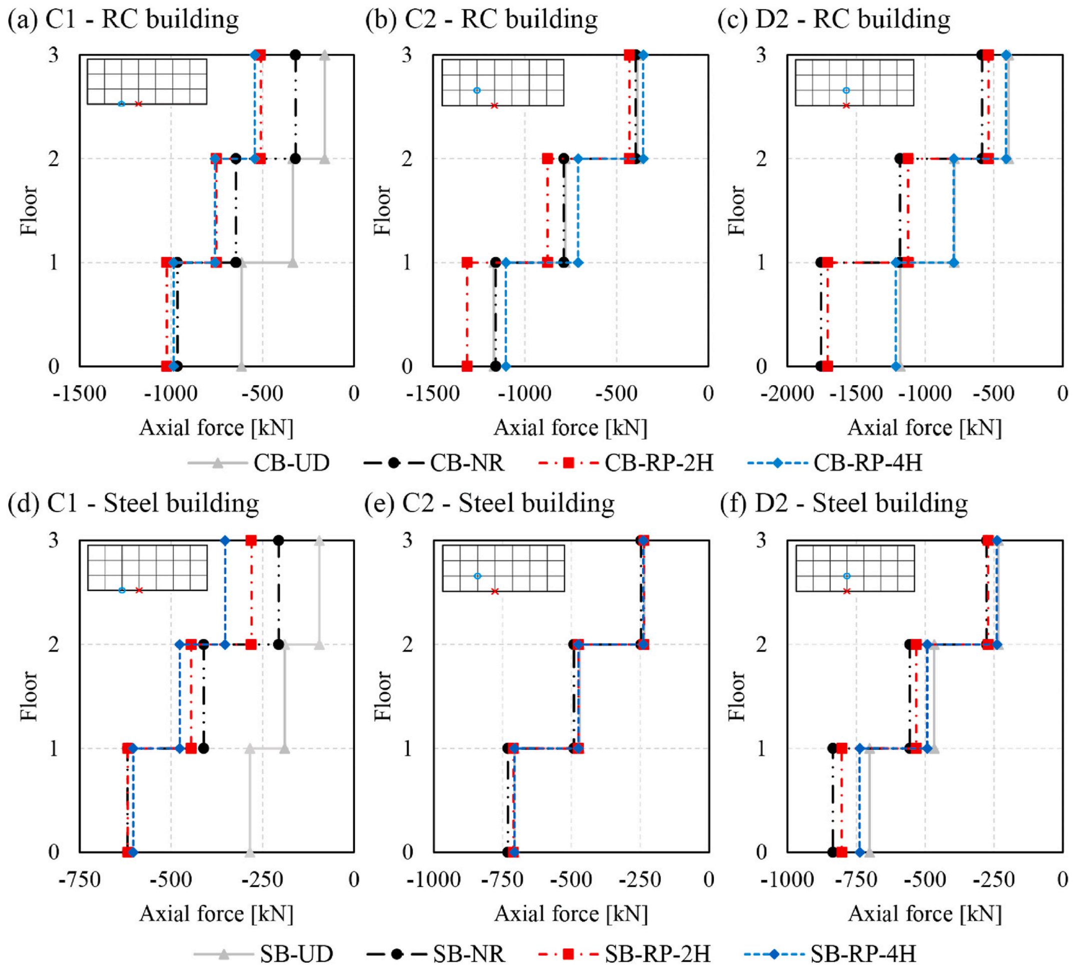

Fig. 10. Axial force in the columns of different alignments: (a) Alignment C1 of the RC building; (b) Alignment C2 of the RC building; (c) Alignment D2 of the RC building; (d) Alignment C1 of the steel building; (e) Alignment C2 of the steel building; (f) Alignment D2 of the steel building.

element (see Fig. 10b and e), the comparison between the undamaged building (UD) and the non-retrofitted one (NR) shows a very small variation in axial force, which is even negligible in the concrete building (Fig. 10b). This indicates that, in the absence of retrofitting, the loads previously carried by element D1.1 are redistributed almost exclusively towards alignments C1 and D2. With the inclusion of the RP-2H retrofit, a significant increase in compressive force is observed in alignment C2 in the RC building (Fig. 10b). Furthermore, an increase in load is observed from the upper to the lower storeys, in contrast to what was seen in alignment C1 (Fig. 10a). The load that was previously observed to dissipate in C1 from the upper to the lower storeys is gradually transferred storey by storey to C2 through the beams, which highlights the importance of 3D modelling in the study of alternative load paths. The RP-4H retrofit, on the other hand, reduces the axial force in the columns of alignment C2, even reaching values lower than those observed in the undamaged building. This behaviour is explained by the fact that increasing the stiffness of the retrofit beam can modify the alternative load path, redistributing part of the load towards columns located farther from the removed column, thereby reducing the demand on the closer ones. This trend is evident in columns B1 and F1 in Figs. 7 and 8 where vertical reaction forces increase with the amount of retrofitting. In the steel structure (Fig. 10e), only a minimal difference is observed in the compressive forces acting on these columns across storeys for the different studied cases. This is attributed to the weak connection between the beam and column in the Y-direction (see Fig. 1). In the steel building, load distribution occurs primarily through the elements located within the strong axis of the structure (X-direction).

In addition to the observations discussed above, a notable difference emerges when comparing the RC and steel buildings: in the steel structure, the columns along alignment C1 (Fig. 10d) experience a greater variation in axial forces than those in the RC buildings. Conversely, as previously discussed, the interior columns C2 and D2 (Fig. 10e and f) show only minor variations across the different buildings studied, in contrast with the behaviour observed in the concrete structures. As noted in Section 4.2.2, this is attributed to the more limited load distribution in the weak axis (Y-direction) of the steel buildings. In contrast, load distribution is more significant along the strong axis of the structure (X-direction).

The results obtained are particularly significant, as they demonstrate that the retrofitting system effectively controls which elements are affected by the failure of a column: in this case, with sufficient perimeter retrofitting at the roof level (such as RP-4H), the involvement of internal columns can be prevented following the failure of a perimeter column.

4.2.5. *Columns far from the damage*

Fig. 11 shows the axial forces at the time step corresponding to the maximum $\delta_{peak,F1}$ in an alignment of columns distant from the damage zone, to which the perimeter retrofit is connected; this corresponds to alignment H1.

In the concrete building, the removal of column D1.1 causes a significant decrease in the axial forces of alignment H1 (see buildings CB-UD and CB-NR in Fig. 11a), exhibiting a seesaw effect towards the removed column. Both retrofitting schemes (RP-2H and RP-4H) manage to redistribute the load towards this column alignment, resulting in an increase in the axial forces in these columns. In the case of RP-4H, the axial force values are higher than those for RP-2H and close to those of the undamaged building. Once again, the RP-4H retrofit proves effective in involving the rest of the structure in resisting the failure of a single element, greatly reducing the seesaw effect observed in the non-retrofitted structure.

In the steel building, however, the corner column H1 is minimally affected. While other perimeter columns experience axial force variations of around 25 % between SB-RP-4H and SB-NR (see vertical base reactions in Fig. 8), the corner column H1 shows a negligible change in axial force (Fig. 11b). This may be attributed to a lower seesaw effect in the steel building compared to the RC building, owing to its higher stiffness, as evidenced by the lower displacements. It is noteworthy that the axial force observed with the RP-4H retrofit in Fig. 11b is identical to that of the undamaged building.

4.2.6. *Retrofit and regular beams*

Another important aspect to address in order to understand the effect of the retrofit beams on the structure is the distribution of internal forces observed in the building's beams. Fig. 12 shows the bending moments in the beams along alignment 1 in the X-direction, both on the first and third floors (the bending moments in the beams on the second floor are not shown due to their similarity to those on the first floor), for the RC building at the time step corresponding to the maximum $\delta_{peak,F1}$. The results are presented simultaneously for the intact building (UD) and for the building after the removal of column D1.1 in the non-retrofitted case (NR), with

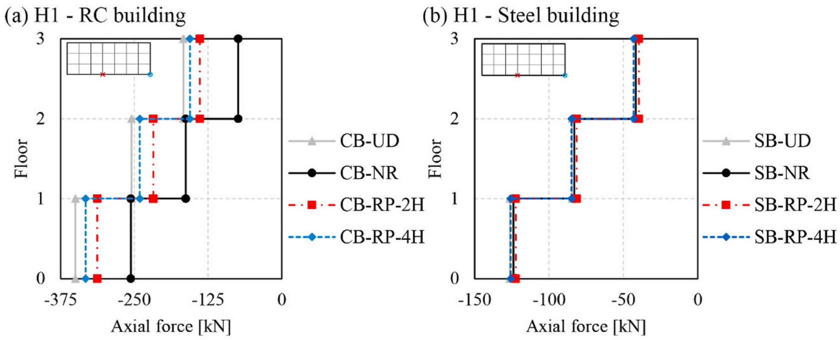

Fig. 11. Axial force in the columns of alignment H1: (a) RC building; (b) Steel building.

the 2H perimeter retrofit (RP-2H), and with the 4H perimeter retrofit (RP-4H). Fig. 13 presents the same results but for the steel building.

In the intact building, the beams in the X-direction behave as continuous beams, exhibiting hogging moments near the supports and sagging moments at mid-span (see the bending moments in the intact buildings (UD) in Fig. 12a and b and Fig. 13a and b). The behaviour of the different floors of the building is analogous under this condition.

The removal of column D1.1 transforms the two spans between alignments C-D and D-E into a single span C-E. This causes a moment reversal in the beams located above D1.1, changing from a hogging bending moment to a significantly high sagging moment (see NR buildings in Figs. 12 and 13). The hogging moment at the joints in alignments C and E increases substantially due to the greater span length that must be supported.

The introduction of retrofit beams leads to significant changes in the internal forces of the beams (see RP-2H and RP-4H buildings in Figs. 12 and 13). The bending moment in the retrofit beams (3rd floor) increases considerably (RP-2H and RP-4H in Figs. 12a and 13a), due to the high stiffness of these elements. The greater the stiffness of the retrofit beam, the higher the bending moment it reaches. This difference is even more pronounced in the steel building, where previous sections have already shown that the RP-4H retrofit produces significant changes compared to the RP-2H retrofit. As a result, the RP-4H retrofit carries a much higher moment than RP-2H (Fig. 13a). The sagging and hogging moments developed in the retrofit beams can be substantially higher compared to the intact building condition. Therefore, the proper performance of the retrofit beams depends on an adequate design of their dimensions (and steel reinforcement, in the case of RC elements) as well as on the connection between the retrofit and existing beams to ensure their strength. It is also worth noting the change in bending behaviour of the beams adjacent to the span affected by the removal of column D1.1 (i.e., beams between alignments B-C and E-F), which become subjected to high hogging moments along their entire length when the RP-4H retrofit is used (see Figs. 12a and 13a).

The moment reversal in the beams of the 3rd floor (from hogging to sagging at mid-span of beam C-E, and from sagging to hogging in beams B-C and E-F) may necessitate strengthening of the existing beam to withstand these demands. For instance, the mid-span of beam C-E in the RC building is likely not reinforced to resist such a large sagging moment, so the existing beam may require strengthening for sagging moments. This should be considered during the retrofitting design phase if the intention is to utilise the existing beam's load-carrying capacity.

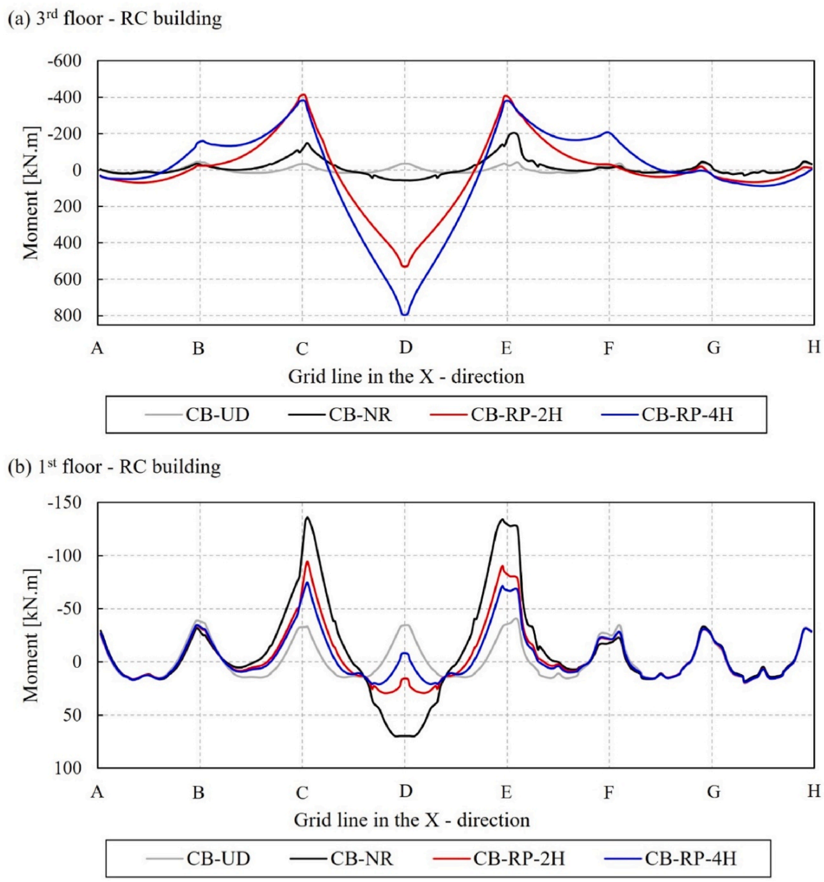

Fig. 12. Bending moments in the beams of the frame located along alignment 1 in the X-direction for the RC building: (a) Third floor beams; (b) First floor beam.

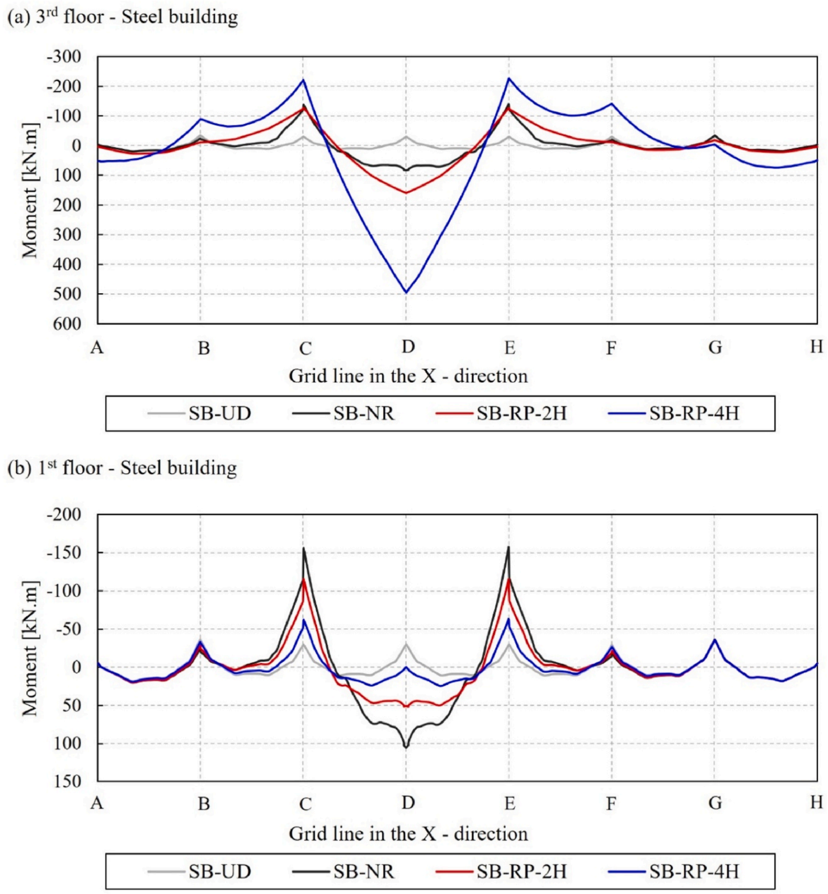

Fig. 13. Bending moments in the beams of the frame located along alignment 1 in the X-direction for the steel building: (a) Third floor beams; (b) First floor beam.

The retrofit beams also have a significant effect on the beams of the other floors in the building. Through the "hanging" effect exerted by the columns located above the removed column (Section 4.2.3), the sagging bending moments on beams C-D and D-E are notably reduced (see RP-2H and RP-4H in Figs. 12b and 13b), reaching bending values similar to those of the intact building (UD) when the retrofit is highly effective (RP-4H). Additionally, the hogging moment near the columns at alignments C and E is greatly diminished compared to the non-retrofitted case. Therefore, the implementation of an effective retrofit at the roof level would contribute significantly to ensuring that the beams meet the required capacity to satisfy the alternative load paths.

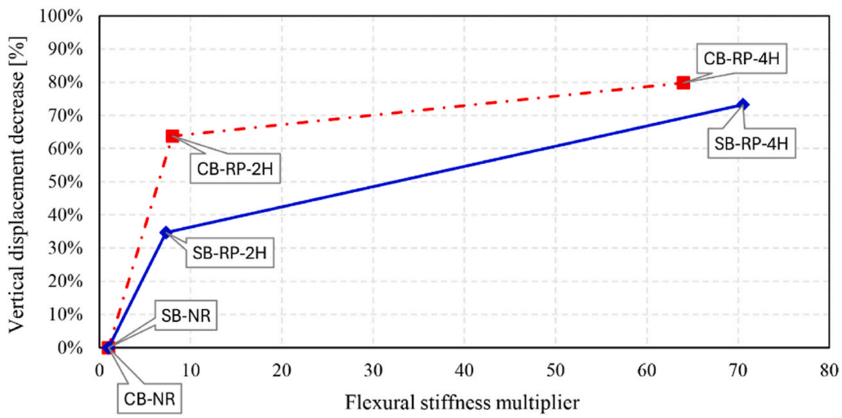

Fig. 14. Percentage decrease of the vertical displacement at the node located above the removed column on the first floor with respect to the non-retrofitted building over the relative increase in the moment of inertia of the top-floor beam regarding the original section.

It should be noted that the beams did not develop catenary action under the applied loads considered in this study in any of the buildings.

4.3. Global analysis of the structural behaviour

After completing the detailed analysis of all critical elements under the selected damage scenario, this section presents a summary of the obtained results. The discussion is structured around the evaluation of the effectiveness of the retrofit beams and concludes with a general description of the structural behaviour of the retrofit beams.

First, the maximum displacements at the node located above the removed column showed a significant reduction in both RC and steel buildings when the retrofit beams were placed (see Section 4.2.1), with the effect becoming more pronounced as the retrofit is increased. To provide a different perspective on the effectiveness of the intervention in relation to the amount of retrofitting required, Fig. 14 plots the percentage reduction in displacement (regarding the non-retrofitted case) as a function of the increase in the moment of inertia of the top-floor beam relative to that of the original beam.

Fig. 14 shows that the 2H profiles result in an increase in the moment of inertia by a factor of 8 and 7.3 compared to the original beam for the RC and steel buildings, respectively. These increases correspond to displacement reductions of 63.8 % and 34.7 % for the RC and steel buildings, respectively. It is evident that, despite similar inertia ratios, the resulting displacement differences between the two cases are significant. When analysing the 4H retrofit, which involves an increase in inertia by factors of 64 and 70 for the RC and steel buildings, respectively, the displacement reductions become comparable, reaching 79.8 % and 73.2 %, respectively. This indicates a highly non-linear trend and reveals a range of optimal retrofit stiffness, in which increasing the amount of retrofitting leads to a substantial gain in overall system rigidity.

To better understand the mechanisms behind these displacement reductions, it is useful to examine how the retrofitting alters the internal force redistribution within the structure. Moreover, by comparing these demands with the theoretical capacities of the critical elements involved in the alternative load path, the effectiveness of the proposed retrofitting in preventing damage propagation can be further assessed.

As shown in the previous sections, the retrofit beams play a key role when a load-bearing element fails by absorbing the loads from the structure and redistributing them globally throughout the building. Within this alternative load path, several critical elements are essential to its development, including the columns located above the removed one, the adjacent columns, and the beams and floors above the removed column. The following analysis focuses on the changes in internal forces experienced by these elements in each case, summarising the findings of Section 4.2, and compares them to their theoretical capacities. For the steel structure, the capacities were calculated following the provisions of EN 1993-1-1:2013 [44], adopting conservative assumptions regarding the reduction of maximum strength due to buckling. In the case of RC, the interaction diagrams were obtained using the software Response 2000 [45].

The columns located above the removed column act as tension ties, transferring loads from the area of the removed column to the retrofit beam. As was observed in Section 4.2.3, increasing the amount of retrofitting leads to higher tensile demand in these elements. However, this increased demand has different implications for the RC and the steel buildings. As shown in Fig. 15, while in the steel building the rise in tensile forces further distances the beam from its capacity limit, in the RC building, the increase in retrofitting leads the element to operate in a demand range very close to its capacity threshold. Consequently, this aspect becomes critical and must be carefully assessed in RC buildings incorporating retrofit beams.

The increase in tensile forces in these columns, resulting from a higher level of retrofitting, leads in turn to a significant reduction in the demand on the building's beams and floors, particularly those above the removed column. This is an essential aspect of this retrofitting technique, as these elements would be otherwise close to reaching their capacity under a local failure scenario. Fig. 16

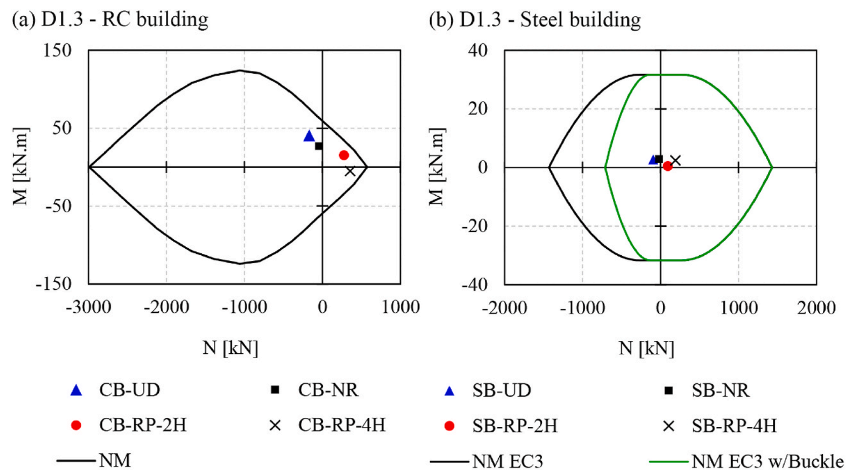

Fig. 15. Demand in the third-floor column above the removed one (column D1-3) compared to the theoretical capacity of the element for the following cases: (a) RC building; (b) Steel building.

shows the demand and capacity of the beams adjacent to the removed column, specifically on the first floor of the building between the alignments C1 and D1, at both ends of the beam. It should be noted that the nominal capacity accounts for the axial force present in each case. However, in the case of the steel beam, no adjustment to the theoretical capacity is required for the axial forces experienced. As observed in Fig. 16a, in the non-retrofitted RC building, both beam ends exceed their nominal capacity: a flexural-shear failure is expected at the C1 end, and a pure flexural failure at the D1 end. However, as the stiffness of the retrofit beam increases, the demand on this element is reduced, keeping it below its nominal capacity. In the case of the steel building, a similar reduction in demand can be observed as the amount of retrofitting increases. However, in all cases, the beam exhibits a capacity significantly higher than the experienced demand.

The retrofit beams also serve to reduce the demand on the interior columns, particularly the one adjacent to the removed column, by transferring the load to the perimeter columns. Fig. 17 shows the demand and capacity of the column D2-1 for each analysed building. As shown, the demand in this interior column in the non-retrofitted RC building is relatively high compared to its capacity, but it decreases significantly as the amount of retrofitting increases. This effect is less noticeable in the steel building, where the force transmission in the shorter direction (Y), which contains the weak connections, is lower (as observed in Section 4.2.2).

The load absorbed by the retrofit beam, which relieves the interior column and the beams and floors (primarily the ones adjacent to the removed column), is subsequently redistributed among the various perimeter columns. As shown in Figs. 18 and 19, columns C1-1 and B1.1 exhibit an increase in demand, more noticeable in C1-1 than in B1.1, although in all cases the values remain well below their theoretical capacity limits. These results support the conclusion that the retrofit beams effectively relieve the demand on critical elements that, in a non-retrofitted building, may be close to their capacity and typically trigger collapse. Instead, the loads are more evenly redistributed to elements that remain well below their theoretical capacity.

Through the analysis carried out, a general understanding is reached of how the retrofitting system using roof beams behaves in response to the failure of an exterior load-bearing element. In the original, non-retrofitted building, the failure of column D1.1 causes a load redistribution towards the adjacent column alignments; specifically, towards both neighbouring columns on the building façade

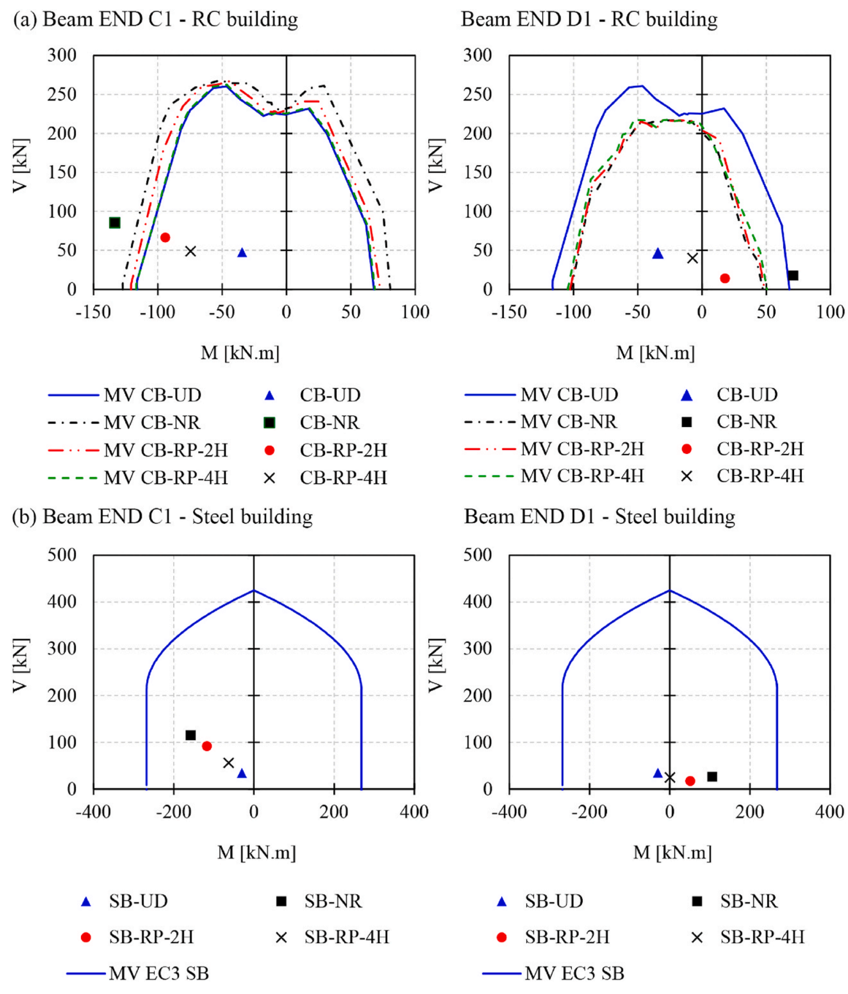

Fig. 16. Demand at both ends of the beam adjacent to the removed column (beam C1-D1) compared to the theoretical capacity of the element for the following cases: (a) RC building; (b) Steel building.

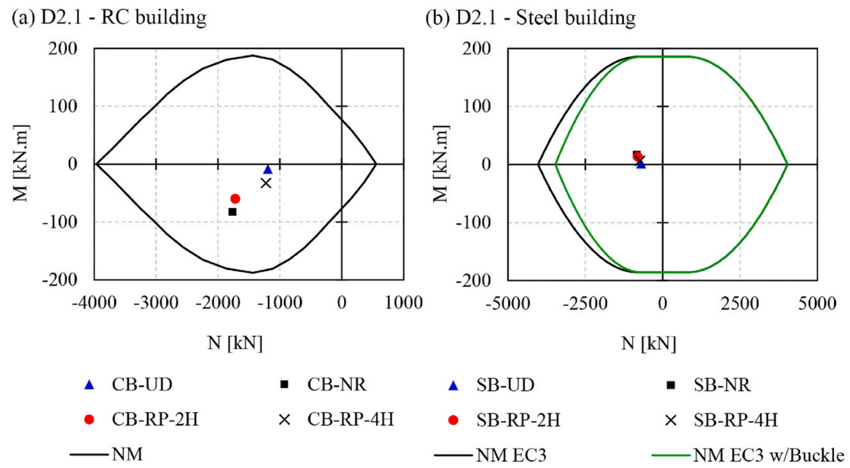

Fig. 17. Demand in the interior column adjacent to the removed one (D2-1) compared to the theoretical capacity of the element for the following cases: (a) RC building; (b) Steel building.

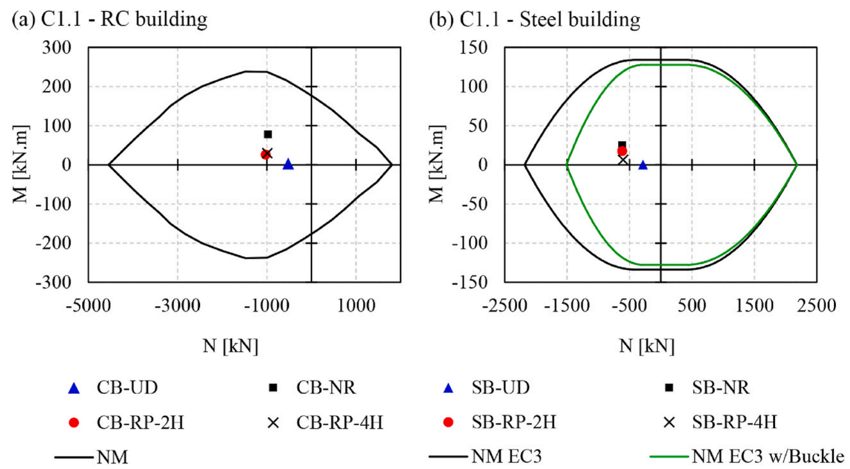

Fig. 18. Demand in the perimetral column C1-1 compared to the theoretical capacity of the element for the following cases: (a) RC building; (b) Steel building.

(C1 and E1) and towards the interior column located perpendicular to the façade (D2). This structural response is illustrated in the sketch shown in Fig. 20a.

A sufficiently stiff perimeter retrofit at the roof level, such as the RP-4H studied, manages to "hang" the slabs after the failure of column D1.1. The columns located above this column act as a tension tie, transferring the load to the rigid beams at the roof level. These beams redistribute the load to other column alignments in the building perimeter; not only to the alignments adjacent to the failed column (C1 and E1) but also to others further away from the failure, such as lines B1 and F1, as well as other column alignments located at the building perimeter. In contrast, the column alignments located within the building interior no longer receive additional load after the failure of D1.1, but rather receive similar or even lower loads than those experienced when the structure is intact. This response is illustrated in Fig. 20b. Moreover, the tension tie behaviour of the columns above the removed column causes the beams on the lower floors, which typically trigger collapse, to exhibit stresses more similar to those of an intact building.

In conclusion, the retrofit beams at the roof level prove effective in preventing collapse. They not only support and redistribute the weight of the structure after the local failure of an element, but also control the direction in which loads are diverted in the event of such failure. This helps to prevent certain structural elements from being involved in the building's load-resisting system. Consequently, it enables prioritisation of those elements of the existing structure that require inspection to ensure the proper functioning of the proposed retrofitting system.

In steel buildings, where strong connections are typically found in certain frame planes and weak connections in others, some differences are observed depending on the arrangement of strong and weak frames. Load redistribution will be more effective in the strong planes than in the weak ones, which should be taken into account in the retrofitting design.

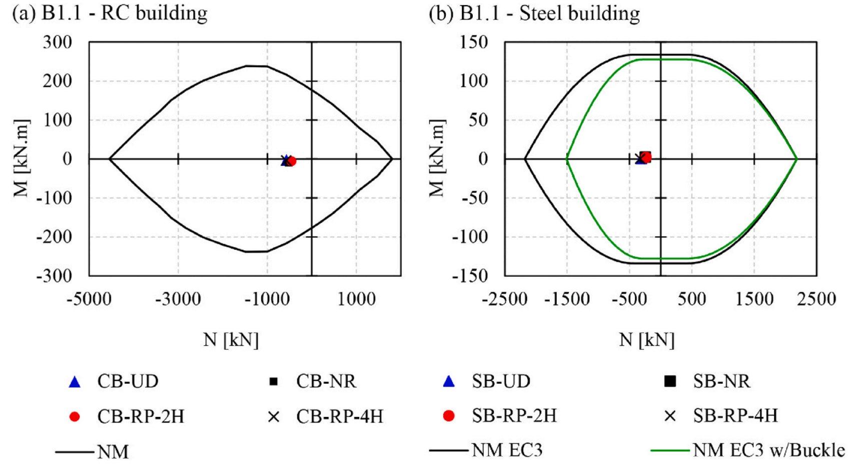

Fig. 19. Demand in the perimetral column B1-1 compared to the theoretical capacity of the element for the following cases: (a) RC building; (b) Steel building.

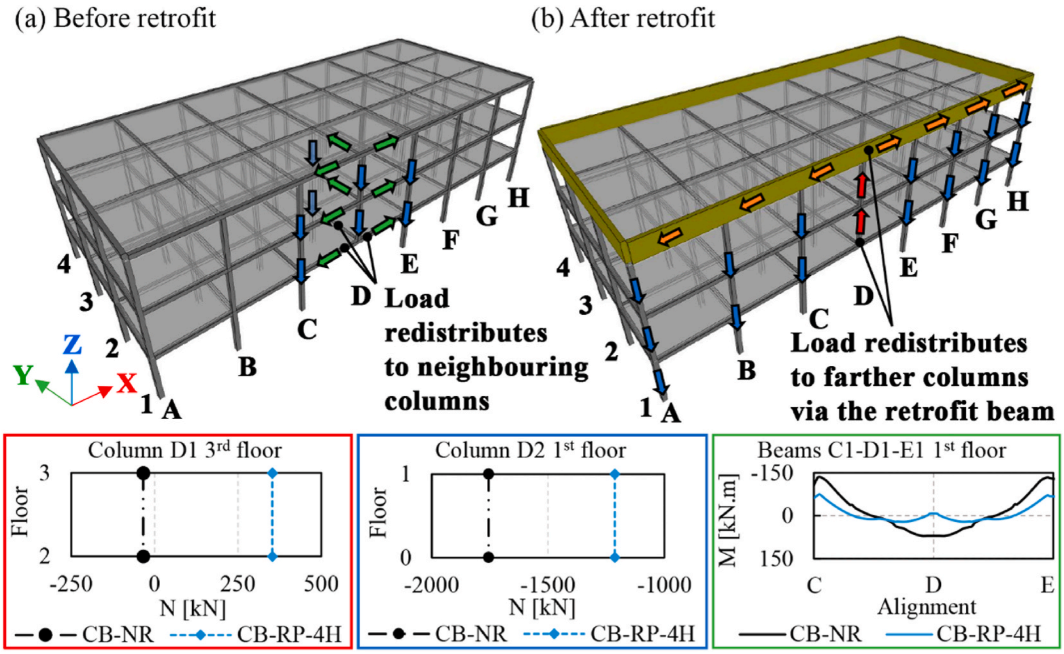

Fig. 20. Sketch of the building's response to the failure of an exterior column at the centre of the long side: (a) Non-retrofitted building (CB-NR); (b) Building with retrofit beams at the roof perimeter (CB-RP-4H).

5. Evaluation of different scenarios

This section evaluates the performance of the retrofit beams under alternative failure scenarios, aiming to assess their effectiveness. To this end, the failure scenario analysed in Section 4 is re-examined with different retrofit beam configurations. In addition, two additional failure scenarios are considered, which involve changes in the configuration and dimensions of the roof beams in both the RC and steel buildings.

As in the previous section, the failure scenarios analysed are defined following the recommendations of the UFC guidelines. In this case, a corner column removal scenario (A1.1) and an interior column removal scenario (D2.1) are proposed (see Fig. 1a). Additionally, the effectiveness of the retrofit beam is assessed by varying its layout in plan (see Fig. 3) and its cross-section (see Fig. 2b). The proposed plan configurations include a perimeter arrangement, as analysed in Section 4 (RP); a perimeter arrangement combined with longitudinal alignments (RX); and a perimeter arrangement combined with transverse alignments (RY). Regarding the cross-sections, retrofit beams are proposed to achieve depths equal to twice (2H) and four times (4H) the height of the original beam, following the same approach used in Section 4.

To quantify the performance of each proposed alternative and damage scenario, the peak vertical displacements at the removed column location, denoted as $\delta_{peak,F1}$, were obtained for all cases, since, as previously noted, this is a good indicator of the demand on the storeys. These are presented in Table 2. Furthermore, Fig. 21 shows the percentage reduction in displacement at the removed column compared to the non-retrofitted state (NR). When comparing the displacements in the structures with retrofit beams to the non-retrofitted case, a significant reduction is observed in most cases. The only exception is the perimeter retrofit configuration under the interior damage scenario (D2.1), where no substantial improvement is achieved, even when using the 4H beam depth.

An improvement in structural response in the interior damage scenario is observed when the RX and RY configurations are implemented, with the former exhibiting a slightly greater enhancement than the latter. This behaviour may be attributed to the increased effectiveness of the retrofit as its length increases, that is, the longer the alignment along which the retrofit beam is placed, the more effective it becomes, as it can rely on a greater number of columns to transfer and redistribute the loads.

Regarding the exterior column scenarios (A1.1 and D1.1), the performance of the different retrofit beam configurations (RP, RX, and RY) does not vary significantly, even when a retrofit beam in the Y-direction reaches the D1.1 column. The UFC guidelines allow for ensuring building robustness against the failure of exterior elements only, particularly when access to the building's interior is restricted and when columns vulnerable to explosions, impacts, or similar hazards are limited to the building perimeter. In such cases, the perimeter retrofit alone is sufficient and likely the most effective solution to enhance the structural response. These scenarios show substantial reductions in displacement, up to 80 % in the RC building and 87 % in the steel building, particularly with the 4H retrofit beams. While it is evident that, especially in the steel structure, the 4H reinforcement performs better than the 2H configuration, a risk-based cost-benefit analysis should be carried out when designing retrofit solutions for real structures in order to select the optimal beam cross-section.

As previously mentioned, the performance of the different configurations under the removal of a perimeter column does not vary significantly. However, it is worth highlighting a minor difference between the steel and RC structures. When comparing the behaviour of the RX and RY reinforcements under the D1.1 column removal scenario, a slightly better performance can be observed for the RY layout in the steel structure, whereas both configurations yield nearly identical results in the RC structure. This difference can be attributed to the lack of bending moment continuity in the Y-direction of the steel building. Installing the retrofit beam in the Y-direction enables stress transfer through flexural action in a direction that was previously inactive, as flexural response was originally limited to the X-direction. In contrast, the RC structure exhibits flexural action in both directions even before retrofit, so the addition of a retrofit beam has a more limited impact on the structure's performance.

6. Conclusions

This study examined the behaviour and effectiveness of roof-level retrofit beams as a strategy to improve the robustness of existing reinforced concrete (RC) and steel buildings. Nonlinear dynamic simulations of representative structures demonstrated that properly dimensioned and configured retrofit beams significantly enhance structural performance and load redistribution in low-rise buildings. The main findings are.

1. Retrofit beams act primarily by modifying alternative load paths (ALPs). By redirecting loads directly to the connected columns, which typically are well below their capacity in accidental situations, they reduce the demand on adjacent non-connected columns and control which elements are affected.
2. Columns above a failing column behave as tension ties, transferring loads to the retrofit beams. This makes assessing their tensile strength crucial, since highly rigid beams may exceed this load path's capacity.
3. Column failure causes moment reversal in the beams above, from a hogging bending moment to a significantly high sagging moment. In retrofitted structures, the tension in columns above the failing one substantially reduces demands on beams and slabs

Table 2
$\delta_{peak,F1}$ displacement for all considered scenarios [units: mm].

	Concrete Building (CB)			Steel Building (SB)		
	A1.1	D1.1	D2.1	A1.1	D1.1	D2.1
NR	−122.4	−116.0	−132.9	−73.7	−34.0	−33.5
RP-2H	−63.3	−42.0	−129.5	−39.4	−22.2	−33.3
RP-4H	−30.8	−23.4	−125.3	−9.4	−9.1	−32.4
RX-2H	−62.5	−41.5	−108.5	−39.2	−22.3	−28.7
RX-4H	−29.3	−23.6	−73.4	−9.8	−8.8	−15.2
RY-2H	−63.4	−40.6	−113.8	−40.4	−21.4	−30.0
RY-4H	−30.3	−23.7	−79.8	−9.6	−8.1	−15.5

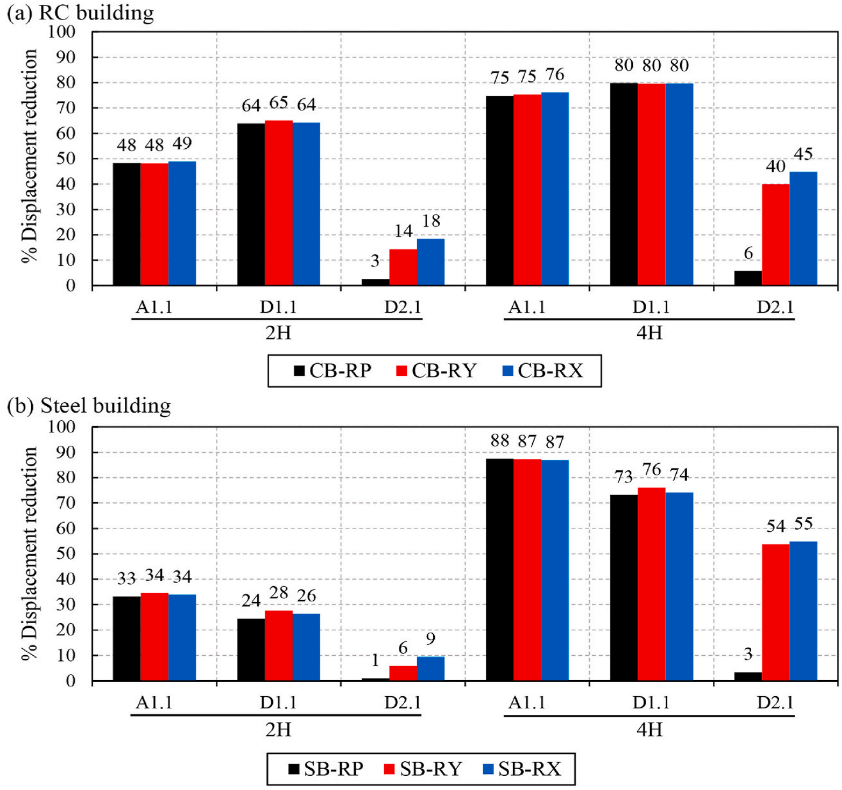

Fig. 21. Percentage reduction of the peak displacement $\delta_{peak,F1}$ for all considered retrofit configurations with respect to the non-retrofitted building: (a) RC building; (b) Steel building.

near the failure. This is a crucial aspect of the retrofitting technique, since these elements are typically close to their capacity under local failure scenarios and often act as the triggers of progressive collapse.

4. Retrofit beams experience significantly high internal forces. Their effectiveness depends on adequate design of their dimensions (and steel reinforcement, in RC elements) and the connection between the retrofit and existing beams. Retrofit beams may exhibit high depth-to-width ratios, so particular attention should be devoted to their design in order to prevent premature instability.
5. In steel buildings, where strong connections are typically found in certain frame planes and weak connections in others, load redistribution is more effective in strong frame planes than in weak ones, which must be considered in retrofit design.
6. The dynamic analysis of displacements revealed that increasing top-floor stiffness may alter vibration frequencies and can induce dynamic decoupling between floors. This decoupling typically arises when the stiffness of the retrofit beam approaches the threshold beyond which additional retrofit becomes ineffective. This behaviour may cause unexpected peaks in reactions or displacements at specific locations, which must be verified in the retrofit design.
7. Perimeter retrofitting alone is ineffective against failures of interior columns. Alternative layouts (such as RX and RY, studied in this paper) are preferable, with RY performing slightly better in the steel building due to weak Y-direction connections, while the RC building showed similar performance in both configurations.

The proposed retrofitting strategy has been conceptually demonstrated to be effective for RC and steel low-rise buildings. However, further research is needed regarding its application to taller buildings, considering the variation of column sizes along the height, or to buildings with higher ductility in seismic design, among other possible parameters. Another important issue to be addressed in future work is the detailed design of the connection between the retrofit beams and the existing structure, which may require strengthening the existing beam to ensure adequate capacity.

CRediT authorship contribution statement

Lisbel Rueda-García: Writing – review & editing, Writing – original draft, Visualization, Validation, Supervision, Software, Methodology, Investigation, Formal analysis, Data curation. **Brais Barros:** Writing – review & editing, Writing – original draft, Visualization, Validation, Supervision, Software, Methodology, Investigation, Formal analysis, Data curation. **Marcos Arias-Gracey:** Writing – original draft, Visualization, Validation, Software, Investigation, Formal analysis, Data curation, Writing – review & editing. **Juan Sebastián Fontalvo-García:** Writing – original draft, Visualization, Validation, Software, Investigation, Formal analysis, Data curation, Writing – review & editing. **Manuel Buitrago:** Writing – review & editing, Supervision, Investigation, Conceptualization, Methodology. **Jose M. Adam:** Writing – review & editing, Supervision, Resources, Funding acquisition, Conceptualization, Methodology.

Declaration of competing interest

The authors declare that they have no known competing financial interests or personal relationships that could have appeared to influence the work reported in this paper.

Acknowledgements

The authors gratefully acknowledge the financial support provided by the Generalitat Valenciana through the ENHANCE project (CIPROM/2022/47), the First Research Projects Grant (PAID-06-24) from the Research Vice-Rectorate of the Universitat Politècnica de València (UPV), and the funding for open access charge provided by CRUE-Universitat Politècnica de València.

Appendix A. Supplementary data

Supplementary data to this article can be found online at https://doi.org/10.1016/j.jobe.2025.114381.

Data availability

All data necessary to reproduce the findings of this study are included in the article and its Supplementary Materials. Further data may be made available upon reasonable request.

References

[1] CRED UNDRR, The Human Cost of Disasters: an Overview of the Last 20 Years (2000-2019), 2020.
[2] N. Makoond, A. Setiawan, M. Buitrago, J.M. Adam, Arresting failure propagation in buildings through collapse isolation, Nature 629 (2024) 592–596, https://doi.org/10.1038/s41586-024-07268-5.
[3] J.M. Adam, F. Parisi, J. Sagaseta, X. Lu, Research and practice on progressive collapse and robustness of building structures in the 21st century, Eng. Struct. 173 (2018) 122–149, https://doi.org/10.1016/j.engstruct.2018.06.082.
[4] J.M. Russell, J. Sagaseta, D. Cormie, A.E.K. Jones, Historical review of prescriptive design rules for robustness after the collapse of Ronan point, Structures 20 (2019) 365–373, https://doi.org/10.1016/j.istruc.2019.04.011.
[5] C. Pearson, N. Delatte, Ronan point apartment Tower collapse and its effect on building codes, J. Perform. Constr. Facil. 19 (2005) 172–177, https://doi.org/10.1061/(ASCE)0887-3828(2005)19:2(172.
[6] I. Azim, J. Yang, S. Bhatta, F. Wang, Q. Liu, Factors influencing the progressive collapse resistance of RC frame structures, J. Build. Eng. 27 (2020) 100986, https://doi.org/10.1016/j.jobe.2019.100986.
[7] Department of Defense (DoD), UFC 4-023-03: Design of Buildings to Resist Progressive Collapse, 2024. http://dod.wbdg.org/.
[8] GSA, Alternate Path Analysis and Design Guidelines for Progressive Collapse Resistance, General Services Administration, Washington DC, USA, 2016.
[9] ASCE/SEI 76-23, Standard for Mitigation of Disproportionate Collapse Potential in Buildings and Other Structures, 2023.
[10] CEN, EN 1990:2023, Eurocode - Basis of Structural and Geotechnical Design, 2023. Brussels.
[11] CEN, EN 1991-1-7, Eurocode 1, Actions on Structures - Part 1-7 General Actions - Accidental Actions, 2018. Brussels.
[12] A. Setiawan, D. Cetina, N. Makoond, M. Buitrago, J.M. Adam, Practical methodology for quantifying the structural robustness of RC building structures, Structures 70 (2024) 107898, https://doi.org/10.1016/j.istruc.2024.107898.
[13] L. Rueda-García, B. Barros, M. Buitrago, J.M. Adam, Robustez estructural de edificios en España. Investigaciones Recientes En La Universitat Politècnica De València, Hormigón Y Acero, 2025, https://doi.org/10.33586/HYA.2025.4044.
[14] L. Possidente, F. Freddi, N. Tondini, Fire response of steel frames retrofitted against progressive collapse, Fire Saf. J. 153 (2025) 104371, https://doi.org/10.1016/j.firesaf.2025.104371.
[15] F. Kiakojouri, V. De Biagi, B. Chiaia, M.R. Sheidaii, Strengthening and retrofitting techniques to mitigate progressive collapse: a critical review and future research agenda, Eng. Struct. 262 (2022) 114274, https://doi.org/10.1016/j.engstruct.2022.114274.
[16] T.M. Pham, H. Hao, Review of concrete structures strengthened with FRP against impact loading, Structures 7 (2016) 59–70, https://doi.org/10.1016/j.istruc.2016.05.003.
[17] S.-Y. Lee, S.-Y. Noh, D. Lee, Comparison of progressive collapse resistance capacities of steel ordinary and intermediate moment frames considering different connection details, Eng. Struct. 231 (2021) 111753, https://doi.org/10.1016/j.engstruct.2020.111753.
[18] L. Zheng, W.-D. Wang, W. Xian, Experimental and numerical investigation on the anti-progressive collapse performance of fabricated connection with CFST column and composite beam, Eng. Struct. 256 (2022) 114061, https://doi.org/10.1016/j.engstruct.2022.114061.
[19] H.M. Elsanadedy, Y.A. Al-Salloum, M.A. Alrubaidi, T.H. Almusallam, H. Abbas, Finite element analysis for progressive collapse potential of precast concrete beam-to-column connections strengthened with steel plates, J. Build. Eng. 34 (2021) 101875, https://doi.org/10.1016/j.jobe.2020.101875.
[20] S. Li, S. Shan, H. Zhang, Y. Li, Rapid retrofit of reinforced concrete frames after progressive collapse to increase sustainability, Sustainability 11 (2019) 4195, https://doi.org/10.3390/su11154195.
[21] K. Qian, B. Li, Strengthening and retrofitting of RC flat slabs to mitigate progressive collapse by externally bonded CFRP laminates, J. Compos. Construct. 17 (2013) 554–565, https://doi.org/10.1061/(ASCE)CC.1943-5614.0000352.
[22] S. Tan, A. Astaneh-Asl, Use of steel cables to prevent progressive collapse of existing buildings, in: Proceedings of Sixth Conference on Tall Buildings in Seismic Regions, 2003. Los Angeles.
[23] A. Naji, M.R. Ommetalab, Horizontal bracing to enhance progressive collapse resistance of steel moment frames, Struct. Des. Tall Special Build. 28 (2019), https://doi.org/10.1002/tal.1563.
[24] J. Jiang, G.-Q. Li, A. Usmani, Effect of bracing systems on fire-induced progressive collapse of steel structures using OpenSees, Fire Technol. 51 (2015) 1249–1273, https://doi.org/10.1007/s10694-014-0451-0.

[25] K. Qian, Y.-H. Weng, B. Li, Improving behavior of reinforced concrete frames to resist progressive collapse through steel bracings, J. Struct. Eng. 145 (2019), https://doi.org/10.1061/(ASCE)ST.1943-541X.0002263.
[26] S.J. Mirvalad, Robustness and Retrofit Strategies for Seismically-Designed Multistory Steel Frame Buildings Prone to Progressive Collapse, Master's Thesis, Concordia University, 2013.
[27] M. Ferraioli, B. Laurenza, A. Lavino, G. De Matteis, Progressive collapse analysis and retrofit of a steel-RC building considering catenary effect, J. Constr. Steel Res. 213 (2024), https://doi.org/10.1016/j.jcsr.2023.108364.
[28] R. Sun, Z. Huang, I.W. Burgess, The collapse behaviour of braced steel frames exposed to fire, J. Constr. Steel Res. 72 (2012) 130–142, https://doi.org/10.1016/j.jcsr.2011.11.008.
[29] S. Jeyarajan, J.Y. Richard Liew, C.G. Koh, Progressive collapse mitigation approaches for steel-concrete composite buildings, International Journal of Steel Structures 15 (2015) 175–191, https://doi.org/10.1007/s13296-015-3013-5.
[30] F. Freddi, L. Ciman, N. Tondini, Retrofit of existing steel structures against progressive collapse through roof-truss, J. Constr. Steel Res. 188 (2022) 107037, https://doi.org/10.1016/j.jcsr.2021.107037.
[31] S.M. Zahrai, A. Ezoddin, Cap truss and steel strut to resist progressive collapse in RC frame structures, Steel Compos. Struct. 26 (2018) 635–647, https://doi.org/10.12989/scs.2018.26.5.635.
[32] M.N.S. Hadi, T.M. Saeed Alrudaini, New building scheme to resist progressive collapse, J. Architect. Eng. 18 (2012) 324–331, https://doi.org/10.1061/(ASCE)AE.1943-5568.0000088.
[33] M. Schachter Adaros, R. Smilowitz, Challenges and considerations for the retrofit of existing structures for progressive collapse, J. Perform. Constr. Facil. 29 (2015), https://doi.org/10.1061/(ASCE)CF.1943-5509.0000675.
[34] CEN, EN 1992-1-1:2023, Eurocode 2 - Design of Concrete Structures - Part 1-1: General Rules and Rules for Buildings, Bridges and Civil Engineering Structures, 2023.
[35] CEN, EN 1993-1-1:2022, Eurocode 3 - Design of Steel Structures - Part 1-1, General rules and rules for buildings, Brussels, 2022.
[36] J.A.J. Huber, H. Mpidi Bita, T. Tannert, S. Berg, Finite element analysis of alternative load paths to prevent disproportionate collapse in platform-type CLT floor systems, Eng. Struct. 240 (2021) 112362, https://doi.org/10.1016/J.ENGSTRUCT.2021.112362.
[37] F. Sadek, S. El-Tawil, H.S. Lew, Robustness of composite floor systems with shear connections: modeling, simulation, and evaluation, J. Struct. Eng. 134 (2008) 1717–1725, https://doi.org/10.1061/(ASCE)0733-9445(2008)134:11(1717.
[38] M. Ferraioli, A. Lavino, A. Mandara, Progressive collapse assessment and retrofit of a multistory steel braced office building, International Journal of Steel Structures 22 (2022) 1086–1107, https://doi.org/10.1007/s13296-022-00626-x.
[39] Computers and Structures Inc., SAP2000 Integrated Software for Structural Analysis and Design, 2024.
[40] G. Mucedero, E. Brunesi, F. Parisi, Nonlinear material modelling for fibre-based progressive collapse analysis of RC framed buildings, Eng. Fail. Anal. 118 (2020) 104901, https://doi.org/10.1016/j.engfailanal.2020.104901.
[41] DIANA FEA BV, DIANA Finite Element Analysis - DIANA Documentation, 2025.
[42] A.K. Chopra, Dynamics of Structures: Theory and Applications to Earthquake Engineering, fifth ed., Pearson Education, 2017.
[43] N. Makoond, M. Buitrago, J.M. Adam, Tests on a full-scale precast building for robustness assessment, in: Structures Congress 2023, American Society of Civil Engineers, 2023, pp. 10–20, https://doi.org/10.1061/9780784484777.002. Reston, vol. A.
[44] CEN, EN 1993-1-1:2013, Eurocode 3: Design of Steel Structures - Part 1-1, General rules and rules for buildings, 2014.
[45] E. Bentz, Sectional Analysis of Reinforced Concrete Members, University of Toronto, 2000.